

000 001 002 003 004 005 FEDMUON: FEDERATED LEARNING WITH BIAS- 006 CORRECTED LMO-BASED OPTIMIZATION 007 008 009

010 **Anonymous authors**
011 Paper under double-blind review
012
013
014
015
016
017
018
019
020
021
022
023
024

ABSTRACT

025 Recently, a new optimization method based on the linear minimization oracle
026 (LMO), called Muon, has been attracting increasing attention since it can train
027 neural networks faster than existing adaptive optimization methods, such as Adam.
028 In this paper, we study how Muon can be utilized in federated learning. We first
029 show that straightforwardly using Muon as the local optimizer of FedAvg does
030 not converge to the stationary point since the LMO is a biased operator. We then
031 propose FEDMUON that can mitigate this issue. We also analyze how solving
032 the LMO approximately affects the convergence rate and find that, surprisingly,
033 FEDMUON can converge for any number of Newton-Schulz iterations, while it
034 can converge faster as we solve the LMO more accurately. Through experiments,
035 we demonstrated that FEDMUON can outperform the state-of-the-art federated
036 learning methods.
037

1 INTRODUCTION

038 Federated learning, which can train neural networks in parallel across many clients, has been attracting
039 much attention (Kairouz et al., 2021; McMahan et al., 2017; Karimireddy et al., 2020). In federated
040 learning, each client has its own training datasets and updates its parameters using a local optimizer,
041 such as SGD. The central server collects the parameters from the clients and aggregates them. Since
042 clients do not need to share their local training datasets with others, federated learning inherently
043 preserves data privacy.
044

045 For training neural networks efficiently, using an appropriate stepsize is one of the most critical
046 factors. If the stepsize is too large, the training collapses, whereas if the stepsize is too small, the
047 training requires a huge number of iterations. To adjust the stepsize on the fly during the training,
048 using adaptive optimization methods, such as AdaGrad (Duchi et al., 2011), Adam (Kingma & Ba,
049 2017), Shampoo (Gupta et al., 2018), and other methods (Loshchilov & Hutter, 2019; Vyas et al.,
050 2025), have long been regarded as the de facto standard for training neural networks.
051

052 Recently, Muon (Liu et al., 2025a) has emerged as a promising alternative, attracting significant
053 attention. Many papers evaluated the performance of Muon and demonstrated that Muon can train
054 neural networks faster and achieve higher accuracy than the existing optimization methods, such as
055 AdamW (Liu et al., 2025a; Semenov et al., 2025). Roughly speaking, Muon projects the momentum
056 in the Momentum SGD onto the space of orthogonal matrices. Muon is closely related to various
057 optimization methods: it can be interpreted as a simplified version of Shampoo (Gupta et al., 2018),
058 in which a certain momentum accumulation is disabled (Liu et al., 2025a), and as an instance of
059 optimizers with linear minimization oracle (LMO) under a specific norm (Pethick et al., 2025).
060 Kovalev (2025) also showed that Muon is a special instance of the trust-region optimization method.
061

062 To use Muon for the large-scale training, developing the distributed version of Muon is important.
063 However, Muon requires us to solve the LMO every iteration, which makes it difficult to straight-
064 forwardly use Muon in a distributed environment. Ahn et al. (2025) proposed a method to solve
065 the LMO in a distributed manner, although their method does not support multiple local steps and
066 incurs a huge communication cost. Thérien et al. (2025) proposed MuLoCo, which extends Muon
067 by allowing clients to update the parameters multiple times by Muon as in Local SGD (Stich, 2019;
068 Woodworth et al., 2020). Although Thérien et al. (2025) demonstrated that MuLoCo performs well
069 when all clients share the same training dataset, their method is limited to homogeneous settings and
070

054 lacks theoretical guarantees. As we show in Section 3, MuLoCo fails to converge when clients have
 055 different datasets, which is a fundamental characteristic of federated learning.
 056

057 In this paper, we study the federated learning methods with the LMO and propose FEDMUON. (i)
 058 First, we show that straightforwardly using Muon as the local optimizer in FedAvg failed to converge
 059 to the stationary point since the LMO is a biased operator. We formally analyze the lower bound of
 060 this straightforward method, showing that it does not converge to the stationary point, especially in
 061 the heterogeneous setting. (ii) We then propose FEDMUON, which can mitigate the bias caused by
 062 the LMO and can provably converge to the stationary point. (iii) Furthermore, we derive a novel
 063 analysis and reveal how the inexact LMO affects the convergence behavior of FEDMUON. Since
 064 solving the LMO exactly is computationally expensive, we solve the LMO approximately by running
 065 the Newton-Schulz iteration (Schulz, 1933) several times in practice. There were many papers that
 066 analyzed the convergence behavior of Muon (Riabinin et al., 2025; Liu et al., 2025a; Shen et al.,
 067 2025), while most of them assumed that the LMO is solved exactly and ignored the effect caused by
 068 the inexact LMO. We analyze the impact of inexact solutions to the LMO on the convergence rate. We
 069 discover that for any number of Newton-Schulz iterations, FEDMUON can converge to the stationary
 070 point and can converge faster by up to a factor proportional to the square root of the dimension of the
 071 parameters as we solve the LMO more accurately. We experimentally demonstrated the effectiveness
 072 of FEDMUON, showing that FEDMUON can achieve higher accuracy than the state-of-the-art adaptive
 073 federated learning optimization methods.
 074

075 Our contributions are summarized as follows:
 076

- 077 • We show that directly plugging Muon into FedAvg as the local optimizer does not converge to the
 078 stationary point since the LMO is a biased operator.
- 079 • We propose FEDMUON, which mitigates the above issue by the bias correction mechanism and
 080 can converge to the stationary point.
- 081 • We analyze the convergence rate of FEDMUON with the inexact LMO. Then, we show that for any
 082 number of Newton-Schulz iterations, FEDMUON can converge, revealing how the Newton-Schulz
 083 iteration affects the convergence rate.
- 084 • Through the experiments, we demonstrated that FEDMUON can outperform the state-of-the-art
 085 federated learning methods.

086 **Notation:** We use $\|\cdot\|$ to denote an arbitrary norm, and its dual norm is denoted by $\|\cdot\|_*$. When
 087 we refer to a specific norm, we explicitly use the notation $\|\cdot\|_p$, $\|\cdot\|_F$, $\|\cdot\|_{\text{sp}}$, and $\|\cdot\|_{\text{trace}}$ to
 088 denote the Schatten p -norm, Frobenius norm, spectral norm, and trace norm, respectively. We denote
 089 $[n] = \{1, 2, \dots, n\}$ for any $n \in \mathbb{N}$.
 090

091 2 PRELIMINARY

092 In this section, we briefly introduce federated learning and Muon. The detailed discussion about the
 093 related works is deferred to Appendix B.
 094

Federated Learning: We consider the following problem where the loss functions are distributed
 095 among n clients:

$$096 \min_{\mathbf{X} \in \mathcal{X}} \left[f(\mathbf{X}) := \frac{1}{n} \sum_{i=1}^n f_i(\mathbf{X}) \right], \quad f_i(\mathbf{X}) := \mathbb{E}_{\xi_i \sim \mathcal{D}_i} [F_i(\mathbf{X}; \xi_i)],$$

096 where \mathcal{X} is the parameter space (e.g., \mathbb{R}^d or $\mathbb{R}^{d_1 \times d_2}$), \mathbf{X} is the model parameter, \mathcal{D}_i is the training
 097 that client i holds, and $f_i : \mathcal{X} \rightarrow \mathbb{R}$ is the loss function of client i .
 098

099 The most fundamental algorithm for federated learning is Federated Averaging (FedAvg) (McMahan
 100 et al., 2017). In FedAvg, each client updates the parameter by using its own loss function, and then
 101 the central server aggregates the parameters sent from the clients. The update rule of FedAvg is
 102 described in Appendix C. The original FedAvg uses SGD as the local optimizer, while, as in the
 103 non-distributed learning, it is important to use adaptive optimization methods for stable and fast
 104 training. Many papers proposed federated learning methods that use more sophisticated optimizers,
 105 such as Momentum SGD (Lin et al., 2021), Adam (Reddi et al., 2021), and the Newton method
 106 (Elgabli et al., 2022). Reddi et al. (2021) proposed a general framework and analyzed the convergence
 107 rate with various optimizers.
 108

108 **Optimizer with Linear Minimization Oracle:** Recently, optimizers with linear minimization
 109 oracle (LMO) have been attracting a lot of attention (Liu et al., 2025a; Pethick et al., 2025; Riabinin
 110 et al., 2025). LMO is defined as follows:

$$111 \quad \text{lmo}(\mathbf{X}; \mathcal{D}) := \arg \min_{\mathbf{Y} \in \mathcal{D}} \langle \mathbf{X}, \mathbf{Y} \rangle,$$

114 where \mathcal{D} is the convex set and $\langle \mathbf{X}, \mathbf{Y} \rangle := \sum_{i,j} X_{ij} Y_{ij}$. Originally, the LMO has been used to solve
 115 the convex constrained problems in the Frank-Wolfe algorithm (Frank & Wolfe, 1956; Jaggi, 2013).
 116 Recently, Jordan et al. (2024) proposed Muon, which uses LMO for training neural networks, which
 117 is an unconstrained optimization problem. They showed that Muon can train neural networks faster
 118 than AdamW (Loshchilov & Hutter, 2019) and Shampoo (Gupta et al., 2018; Shi et al., 2023), which
 119 are the most commonly used optimizers these days.

120 Specifically, the optimizers with LMO choose the unit ball as the constraint set \mathcal{D} , measured in
 121 any chosen norm $\|\cdot\|$. With a slight abuse of notation, we use $\text{lmo}(\cdot)$ to represent $\text{lmo}(\cdot; \mathcal{D})$ with
 122 $\mathcal{D} := \{\mathbf{Y} \in \mathcal{X} \mid \|\mathbf{Y}\| \leq 1\}$, i.e.,

$$123 \quad \text{lmo}(\mathbf{X}) := \arg \min_{\mathbf{Y} \in \{\mathbf{Y} \in \mathcal{X} \mid \|\mathbf{Y}\| \leq 1\}} \langle \mathbf{X}, \mathbf{Y} \rangle.$$

125 Then, the update rules are given by:

$$127 \quad \mathbf{M}^{(r+1)} = (1 - \alpha) \mathbf{M}^{(r)} + \alpha \nabla F(\mathbf{X}^{(r)}; \xi^{(r)}),$$

$$128 \quad \mathbf{X}^{(r+1)} = \mathbf{X}^{(r)} + \eta \text{lmo}(\mathbf{M}^{(r+1)}).$$

130 By varying the norm, we can recover different popular optimizers. Specifically, if parameter space
 131 is a vector when we choose the Euclidean norm and max norm, we can recover Normalized SGD
 132 with momentum (Cutkosky & Mehta, 2020) and Sign SGD with momentum (Sun et al., 2023),
 133 respectively. Then, if the parameter space is $\mathbb{R}^{d_1 \times d_2}$ and we use the spectral norm for the LMO, we
 134 can obtain Muon (Jordan et al., 2024). Note that the parameter space needs to be the space of $d_1 \times d_2$
 135 matrices for Muon. Each layer is taken into account separately. For instance, the parameter of the
 136 convolutional layer is $out_channel \times in_channel \times h \times w$ matrix. When we use Muon, we consider
 137 $d_1 = out_channel$ and $d_2 = in_channel \times h \times w$. The remaining scalar and vector parameters in the
 138 neural network are trained by other optimization methods, such as SGD or Adam.

139 For the remainder of the paper, we will not take separate layers into account and represent all the
 140 model parameters as a single matrix for simplicity of presentation. We refer to Riabinin et al. (2025)
 141 for an explanation of how to take into account every layer separately in the analysis of Muon.

143 3 LOCALMUON DOES NOT ALWAYS CONVERGE

145 First, we provide a lower bound showing that straightforwardly using the optimizer with the LMO
 146 as the local optimizer in FedAvg does not always converge. For simplicity, we consider the setting
 147 where all clients participate in every round and perform exactly one local update. Straightforwardly
 148 applying the optimizer with the LMO to FedAvg yields the following update rules:

$$149 \quad \mathbf{M}_i^{(r+1)} = (1 - \alpha) \mathbf{M}_i^{(r)} + \alpha \nabla F_i(\mathbf{X}^{(r)}, \xi_i^{(r)}), \quad (1)$$

$$151 \quad \mathbf{X}_i^{(r+1)} = \mathbf{X}_i^{(r)} + \eta \text{lmo}(\mathbf{M}_i^{(r+1)}), \quad (2)$$

$$153 \quad \mathbf{X}^{(r+1)} = \frac{1}{n} \sum_{i=1}^n \mathbf{X}_i^{(r+1)}. \quad (3)$$

155 We refer to the above algorithm as LOCALMUON (see Appendix C for LOCALMUON with multiple
 156 local steps and partial participation). However, the above straightforward method fails to reach a
 157 stationary point due to the bias introduced by the LMO, and the optimization process stagnates.
 158 Specifically, the LMO is biased, since in general we have

$$160 \quad \frac{1}{n} \sum_{i=1}^n \text{lmo}(\mathbf{M}_i^{(r+1)}) \neq \text{lmo}\left(\frac{1}{n} \sum_{i=1}^n \mathbf{M}_i^{(r+1)}\right).$$

162 The momentum \mathbf{M}_i is the estimation of the gradient $\nabla f_i(\mathbf{X})$, while the quantity of $\frac{1}{n} \sum_{i=1}^n \text{lm}(\mathbf{M}_i)$
 163 is biased and does not align with the gradient $\nabla f(\mathbf{X})$. This intuitively shows why LOCALMUON
 164 cannot converge to the stationary point, especially when clients have different loss functions. The
 165 following theorem formalizes this failure, with the proof deferred to Appendix D.

166 **Theorem 1.** *For simplicity, we consider the initialization $\mathbf{M}_i^{(0)} = 0$. There exist convex functions
 167 $\{f_i\}_{i=1}^n$ such that for any $r \geq 1$ rounds, the output of LOCALMUON (Eqs. (1) to (3)) is the same as
 168 the initial parameter and does not converge to the optimal solution and satisfies the following:*

$$169 \quad \|\nabla f(\mathbf{X}^{(r)})\|^2 \geq \Omega(\zeta_*^2),$$

170 where $\zeta_*^2 := \frac{1}{n} \sum_{i=1}^n \|\nabla f_i(\mathbf{X}^*)\|^2$ and $\mathbf{X}^* := \arg \min f(\mathbf{X})$.

171 Note that LOCALMUON is a simplified version of MuLoCo (Thérien et al., 2025), where the mo-
 172 mentum at the central server is disabled. We formally analyze only LOCALMUON, while Theorem 1
 173 shows that the parameter stays at the initial parameters and does not converge to the stationary point.
 174 This indicates that MuLoCo also suffers from the same issue, as adding the momentum at the central
 175 server does not prevent the parameter from remaining at its initial value.

178 4 FEDMUON

180 In the previous section, we showed that due to the bias caused by the LMO, LOCALMUON does
 181 always converge. In this section, in Algorithm 1 we propose FEDMUON, which mitigates this issue
 182 and provably converges to the stationary point.

184 Instead of applying the LMO to the momentum alone, we apply the LMO to the bias corrected
 185 version of the momentum (line 8) in Algorithm 1. Similarly to SCAFFOLD (Karimireddy et al.,
 186 2020) we introduce control variates $\mathbf{C}_i^{(r)}$ and $\mathbf{C}^{(r)}$ to estimate the directions of the local client
 187 gradients $\nabla f_i(\mathbf{X}^{(r)})$ and the global gradient $\nabla f(\mathbf{X}^{(r)})$, respectively. Given that the local momentum
 188 parameters $\mathbf{M}_i^{(r,k+1)}$ estimate local gradients $\nabla f_i(\mathbf{X}^{(r,k)})$, the corrected update, $\mathbf{M}_i^{(r,k+1)} - \mathbf{C}_i^{(r)} +$
 189 $\mathbf{C}^{(r)}$ is a good estimation of the full gradient $\nabla f(\mathbf{X}^{(r,k)})$, mitigating the issue of local bias. When
 190 we remove the LMO and set $\alpha = 1$, FEDMUON recovers vanilla SCAFFOLD (Karimireddy et al.,
 191 2020). It is important to note that there are several papers that apply the momentum to SCAFFOLD
 192 (Cheng et al., 2024; Karimireddy et al., 2021), however all of them incorporate momentum at the
 193 central server, differing from our proposed FEDMUON.

195 Algorithm 1 FEDMUON

196 1: **Input:** total number of clients n , number of sampled clients S , and the number of local steps K .
 197 2: **for** $r \in \{0, 1, \dots, R-1\}$ **do** (at the server)
 198 3: sample S clients $\mathcal{S}_r \subset [n]$.
 199 4: send $\mathbf{X}^{(r)}$ and $\mathbf{C}^{(r)}$ to the sampled clients.
 200 5: **for** $i \in \mathcal{S}_r$ **do** (at the clients)
 201 6: $\mathbf{X}_i^{(r,0)} \leftarrow \mathbf{X}^{(r)}$ and $\mathbf{M}_i^{(r,0)} \leftarrow \mathbf{M}_i^{(r-1,K)}$
 202 7: **for** $k = 0, 1, \dots, K-1$ **do**
 203 8: $\mathbf{M}_i^{(r,k+1)} \leftarrow (1-\alpha)\mathbf{M}_i^{(r,k)} + \alpha \nabla F_i(\mathbf{X}_i^{(r,k)}; \xi_i^{(r,k)})$.
 204 9: $\mathbf{X}_i^{(r,k+1)} \leftarrow \mathbf{X}_i^{(r,k)} + \eta \text{lm}(\mathbf{M}_i^{(r,k+1)} - \mathbf{C}_i^{(r)} + \mathbf{C}^{(r)})$.
 205 10: **end for**
 206 11: $\mathbf{C}_i^{(r+1)} \leftarrow \mathbf{M}_i^{(r,K)}$
 207 12: send $\mathbf{X}_i^{(r,K)}$ and $\mathbf{C}_i^{(r+1)}$ to the central server.
 208 13: **end for** (end clients, back to the server)
 209 14: **for** $i \in [n] \setminus \mathcal{S}_r$ **do**
 210 15: $\mathbf{C}_i^{(r+1)} \leftarrow \mathbf{C}_i^{(r)}$ and $\mathbf{M}_i^{(r,K)} \leftarrow \mathbf{M}_i^{(r-1,K)}$.
 211 16: **end for**
 212 17: $\mathbf{C}^{(r+1)} \leftarrow \mathbf{C}^{(r)} + \frac{1}{N} \sum_{i \in \mathcal{S}_r} (\mathbf{C}_i^{(r+1)} - \mathbf{C}_i^{(r)})$.
 213 18: $\mathbf{X}^{(r+1)} \leftarrow \frac{n-S}{n} \mathbf{X}^{(r)} + \frac{1}{n} \sum_{i \in \mathcal{S}_r} \mathbf{X}_i^{(r,K)}$.
 214 19: **end for**

216

5 CONVERGENCE ANALYSIS

217

5.1 ASSUMPTIONS

220 We first summarize the assumptions that we use in our theoretical results. As is common in the prior
 221 literature analyzing optimizers with LMO (Pethick et al., 2025; Riabinin et al., 2025), we use the
 222 following smoothness assumption. Note that the norm here is the same as the one used in the LMO.

223 **Assumption 1.** *There exists $L \geq 0$ so that it holds for any $\mathbf{X}, \mathbf{Y} \in \mathcal{X}$*

$$224 \quad 225 \quad \|\nabla f_i(\mathbf{X}) - \nabla f_i(\mathbf{Y})\|_* \leq L\|\mathbf{X} - \mathbf{Y}\|.$$

226 Since we consider non-Euclidean norms, we measure gradient differences in the dual norm, while
 227 parameter differences are measured in the primal norm (cf. Nesterov, 2018; Xie & Li, 2024). However,
 228 as shown in Remark 1, any two norms are equivalent in finite dimensions, and thus the class of
 229 functions satisfying Assumption 1 and the conventional smoothness assumptions (formulated for
 230 Euclidean norms) is the same (see Remark 2).

231 **Remark 1** ((Conway, 2019, Theorem 3.1)). *If \mathcal{X} is a finite-dimensional vector space over \mathbb{F} , then
 232 for any two norms $\|\cdot\|_p$ and $\|\cdot\|_q$, there exist $c, C \geq 0$ such that $c\|\mathbf{X}\|_p \leq \|\mathbf{X}\|_q \leq C\|\mathbf{X}\|_p$ for
 233 all $\mathbf{X} \in \mathcal{X}$.*

234 **Remark 2.** *If it holds that $\|\nabla f_i(\mathbf{X}) - \nabla f_i(\mathbf{Y})\| \leq CL\|\mathbf{X} - \mathbf{Y}\|$ for any $\mathbf{X}, \mathbf{Y} \in \mathcal{X}$, then
 235 f_i satisfies Assumption 1 where $C := \sup_{\mathbf{X} \in \mathcal{X}} \frac{\|\mathbf{X}\|_*}{\|\mathbf{X}\|}$. If f_i satisfies Assumption 1, it holds that
 236 $\|\nabla f_i(\mathbf{X}) - \nabla f_i(\mathbf{Y})\| \leq \frac{L}{c}\|\mathbf{X} - \mathbf{Y}\|$ for any $\mathbf{X}, \mathbf{Y} \in \mathcal{X}$ where $c := \sup_{\mathbf{X} \in \mathcal{X}} \frac{\|\mathbf{X}\|}{\|\mathbf{X}\|_*}$.*

237 For the analysis of FEDMUON, we often use the trace norm and Frobenius norm. The following
 238 inequality holds between the Frobenius norm and the trace norm.

239 **Example 1.** *For any $\mathbf{X} \in \mathbb{R}^{d_1 \times d_2}$, it holds that $\|\mathbf{X}\|_F \leq \|\mathbf{X}\|_{trace} \leq \sqrt{\min\{d_1, d_2\}}\|\mathbf{X}\|_F$.*

240 For the stochastic gradient noise, we use the following assumption, which is quite common in the
 241 optimization literature, e.g., (Bubeck, 2015).

242 **Assumption 2.** *The stochastic gradient is unbiased, i.e., $\mathbb{E}[\nabla F_i(\mathbf{X}; \xi_i)] = \nabla f_i(\mathbf{X})$ for any $\mathbf{X} \in \mathcal{X}$.
 243 Then, there exists $\sigma \geq 0$ so that it holds for any $\mathbf{X} \in \mathcal{X}$*

$$244 \quad \mathbb{E}_{\xi_i \sim \mathcal{D}_i} \|\nabla F_i(\mathbf{X}; \xi_i) - \nabla f_i(\mathbf{X})\|_F^2 \leq \sigma^2.$$

245

5.2 CONVERGENCE RESULT

246 We provide the convergence rate of FEDMUON in Theorem 2. For simplicity, we present the results
 247 for the special case $S = n$, where all clients participate during the training. The general case with
 248 arbitrary S is provided in Lemma 11 in Appendix E. The proof is deferred to Appendix E.

249 **Theorem 2.** *Consider Algorithm 1. We define $\mathbf{X}^{(r,k)} = \frac{1}{n} \sum_{i=1}^n \mathbf{X}_i^{(r,k)}$. Note that $\mathbf{X}^{(r+1)} =$
 250 $\mathbf{X}^{(r,K)}$. Suppose that $n = S$ and Assumptions 1 and 2 hold, $\mathbf{C}_i^{(0)} := \mathbf{M}_i^{(0,0)}$ and $\mathbf{C}^{(0)} :=$
 251 $\frac{1}{n} \sum_{i=1}^n \mathbf{C}_i^{(0)}$, there exists η and α so that it satisfies*

$$252 \quad \frac{1}{RK} \sum_{r=0}^{R-1} \sum_{k=0}^{K-1} \mathbb{E} \left\| \nabla f(\mathbf{X}^{(r,k)}) \right\|_* \leq \mathcal{O} \left(\left(\frac{Lr_0\tilde{\sigma}^2}{nRK} \right)^{\frac{1}{4}} + \left(\frac{Lr_0\tilde{\sigma}}{R\sqrt{K}} \right)^{\frac{1}{3}} + \left(\frac{Lr_0}{R} \right)^{\frac{1}{2}} \right. \\ 253 \quad \left. + \tilde{\sigma}_0 \left[\frac{1}{R} + \left(\frac{\tilde{\sigma}^2 K}{Lr_0 R n} \right)^{\frac{1}{2}} + \left(\frac{\tilde{\sigma}^2 K^2}{Lr_0 R^2} \right)^{\frac{1}{3}} \right] \right),$$

254 where $r_0 := f(\mathbf{X}^{(0)}) - f^*$, $\rho := \sup_{\mathbf{X} \in \mathcal{X}} \frac{\|\mathbf{X}\|_*}{\|\mathbf{X}\|_F}$, $\tilde{\sigma} := \rho\sigma$, $\tilde{\sigma}_0 := \rho\sigma_0$, and $\sigma_0^2 :=$
 255 $\frac{1}{n} \sum_{i=1}^n \mathbb{E} \|\mathbf{M}_i^{(0,0)} - \nabla f_i(\mathbf{X}^{(0)})\|_F^2$.

256 **Discussion:** Unlike LOCALMUON, Theorem 2 shows that FEDMUON can mitigate the issue that the
 257 LMO is a biased operator and can converge to the stationary point. The dominant term is $\mathcal{O}(\frac{Lr_0\tilde{\sigma}^2}{nRK})^{\frac{1}{4}}$,

270 **Algorithm 2** Newton-Schulz iteration
 271
 272 1: **Input:** matrix \mathbf{G} and hyperparameters $a, b, c \in \mathbb{R}$.
 273 2: $\mathbf{G}^{(0)} \leftarrow \frac{\mathbf{G}}{\|\mathbf{G}\|_F}$.
 274 3: **for** $t \in \{0, 1, \dots, T-1\}$ **do**
 275 4: $\mathbf{G}^{(t+1)} \leftarrow a\mathbf{G}^{(t)} + b(\mathbf{G}^{(t)}\mathbf{G}^{(t)\top})\mathbf{G}^{(t)} + c(\mathbf{G}^{(t)}\mathbf{G}^{(t)\top})^2\mathbf{G}^{(t)}$.
 276 5: **end for**
 277 6: **Retern** $-\mathbf{G}^{(T)}$

278
 279 which is almost the same as the terms appearing in the rate of FedAvg and SCAFFOLD (Karimireddy
 280 et al., 2020), and the convergence rate is improved as the number of clients n increases. The only
 281 difference is that the convergence rate of FEDMUON depends on ρ , while this is because Theorem 2
 282 analyzes the dual norm of the gradient. For instance, when the norm is the Frobenius norm, the dual
 283 norm is also the Frobenius norm and $\rho = 1$. The last three terms arise from the initial error σ_0 , which
 284 diminish faster than the other terms as the number of rounds R increases.
 285

286 We consider the case where the parameter space is $\mathcal{X} = \mathbb{R}^{d_1 \times d_2}$ and the spectral norm is used,
 287 as in Muon (Liu et al., 2025a). Since the dual of the spectral norm is the trace norm, we have
 288 $\|\nabla f(\mathbf{X})\|_F \leq \|\nabla f(\mathbf{X})\|_{\text{trace}}$. Consequently, FEDMUON can converge faster than SCAFFOLD in
 289 certain cases. For instance, if the stochastic noise σ is sufficiently small, FEDMUON converges as:

$$290 \quad \frac{1}{RK} \sum_{r=0}^{R-1} \sum_{k=0}^{K-1} \mathbb{E} \left\| \nabla f(\mathbf{X}^{(r,k)}) \right\|_{\text{trace}} \leq \mathcal{O} \left(\left(\frac{r_0 L}{R} \right)^{\frac{1}{2}} \right),$$

293 and SCAFFOLD converges as follows (see Theorem 3 in (Karimireddy et al., 2020)):

$$294 \quad \frac{1}{RK} \sum_{r=0}^{R-1} \sum_{k=0}^{K-1} \mathbb{E} \left\| \nabla f(\mathbf{X}^{(r,k)}) \right\|_F \leq \mathcal{O} \left(\left(\frac{r_0 L_F}{R} \right)^{\frac{1}{2}} \right).$$

297 where L_F refers to the smoothness of f_i with respect to the Frobenius norm. Thus, when $L =$
 298 $\sup_{i \in [n], \mathbf{X}, \|\mathbf{U}\|_{\text{sp}} \leq 1} \langle \mathbf{U}, \nabla^2 f_i(\mathbf{X}) \mathbf{U} \rangle \approx L_F$, i.e., when the Hessians have a few dominant singular
 299 values—equivalently, when they are approximately low-rank, then FEDMUON can converge faster
 300 than SCAFFOLD. More precisely, the terms on the right-hand side are the same, and the only
 301 difference is the choice of the norm. We stress that Theorem 2 does not claim FEDMUON always
 302 converges faster, but it does suggest that in certain cases FEDMUON can outperform. This helps
 303 explain the strong empirical performance of Muon and FEDMUON.
 304

305 6 FEDMUON WITH INEXACT LMO

307 In the previous section, we considered the general case with an arbitrary norm and exact LMO. Here,
 308 we focus on the spectral norm, as in Muon (Liu et al., 2025a), and analyze FEDMUON when the
 309 LMO is only approximately solved via the Newton–Schulz iteration. Then, thanks to the special
 310 property of spectral norm and Newton–Schulz iteration, we reveal that FEDMUON can converge to
 311 the stationary point regardless of how accurately we solve the LMO.

312 With the spectral norm, the LMO takes the following form:
 313

$$314 \quad \text{lmo}_{\text{muon}}(\mathbf{X}) := \arg \min_{\mathbf{Y} \in \{\mathbf{Y} \in \mathbb{R}^{d_1 \times d_2} \mid \|\mathbf{Y}\|_{\text{sp}} \leq 1\}} \langle \mathbf{X}, \mathbf{Y} \rangle,$$

316 Let the singular value decomposition of \mathbf{X} be $\mathbf{U}\Sigma\mathbf{V}$. Then the LMO output is $-\mathbf{U}\mathbf{V}$, but computing
 317 this exactly is computationally expensive. To address this, Liu et al. (2025a) proposed approximating
 318 the LMO via a fixed number of Newton–Schulz iterations (Schulz, 1933)(e.g., 5). The update rule
 319 of the Newton–Schulz iteration is described in Algorithm 2. Since the procedure involves only
 320 matrix multiplications, it can be efficiently executed on a GPU. In the following, we analyze the
 321 convergence of FEDMUON when the LMO is solved approximately using Newton–Schulz iterations
 322 and characterize how inexactness impacts convergence.
 323

Under the same assumption as in Theorem 2, we provide the convergence rate when we run Newton–Schulz iteration T times to solve the LMO approximately and show how T affects convergence. For

324 simplicity, we set $n = S$ and we use $a = \frac{15}{8}$, $b = -\frac{5}{4}$ and $c = \frac{3}{8}$ for the Newton-Schulz iteration,
 325 following the hyperparameter setting mentioned in Amsel et al. (2025). For the general case of
 326 arbitrary S we refer to Lemma 14 in Appendix F.

327 **Theorem 3.** Consider Algorithm 1 with the spectral norm and suppose that the LMO in line 8 is
 328 solved approximately using Algorithm 2 with $a = \frac{15}{8}$, $b = -\frac{5}{4}$, and $c = \frac{3}{8}$. We define $\mathbf{X}^{(r,k)} =$
 329 $\frac{1}{n} \sum_{i=1}^n \mathbf{X}_i^{(r,k)}$. Note that $\mathbf{X}^{(r+1)} = \mathbf{X}^{(r,K)}$. Suppose that $n = S$ and Assumptions 1 and 2 hold,
 330 $\mathbf{C}_i^{(0)} := \mathbf{M}_i^{(0,0)}$ and $\mathbf{C}^{(0)} := \frac{1}{n} \sum_{i=1}^n \mathbf{C}_i^{(0)}$. Then, for any number of Newton-Schulz iteration $T \geq 0$,
 331 there exists η and α so that it satisfies

$$333 \quad \frac{1}{RK} \sum_{r=0}^{R-1} \sum_{k=0}^{K-1} \mathbb{E} \left\| \nabla f(\mathbf{X}^{(r,k)}) \right\|_p \leq \mathcal{O} \left(\left(\frac{Lr_0 \tilde{\sigma}^2}{nRK} \right)^{\frac{1}{4}} + \left(\frac{Lr_0 \tilde{\sigma}}{R\sqrt{K}} \right)^{\frac{1}{3}} + \left(\frac{Lr_0}{R} \right)^{\frac{1}{2}} \right. \\ 334 \quad \left. + \tilde{\sigma}_0 \left[\frac{1}{R} + \left(\frac{\tilde{\sigma}^2 K}{Lr_0 R n} \right)^{\frac{1}{2}} + \left(\frac{\tilde{\sigma}^2 K^2}{Lr_0 R^2} \right)^{\frac{1}{3}} \right] \right), \\ 335$$

336 where $r_0 := f(\mathbf{X}^{(0)}) - f^*$, $\rho := \sqrt{\min\{d_1, d_2\}}$, $\tilde{\sigma} := \rho\sigma$, $\tilde{\sigma}_0 := \rho\sigma_0$, and $\sigma_0^2 :=$
 337 $\frac{1}{n} \sum_{i=1}^n \mathbb{E} \|\mathbf{M}_i^{(0,0)} - \nabla f_i(\mathbf{X}^{(0)})\|_F^2$. Then, p is defined as follows:

$$338 \quad p := 1 + \frac{\log \left(1 - (1 - \kappa)^{1.5^T} \right)}{\log \kappa}, \\ 339 \quad \kappa := \min_{j,i,r,k} \frac{s_{j,i,r,k}}{\sqrt{\sum_{j'} s_{j',i,r,k}^2}} (> 0), \\ 340 \quad 341$$

342 where $\{s_{j,i,r,k}\}_j$ are non-zero singular values of $\mathbf{M}_i^{(r,k+1)} - \mathbf{C}_i^{(r)} + \mathbf{C}^{(r)}$.

343 **Remark 3.** When $T = 0$, $p = 2$. As T increase, p monotonically decreases to 1 for any $\kappa > 0$.

344 **Remark 4.** Recall that $\|\cdot\|_p$ is the Schatten p -norm. For any $1 \leq p \leq q$, we have $\|\mathbf{A}\|_q \leq \|\mathbf{A}\|_p$.
 345 Then, $\|\mathbf{A}\|_p$ becomes $\|\mathbf{A}\|_{\text{trace}}$ and $\|\mathbf{A}\|_F$ when $p = 1$ and $p = 2$, respectively.

346 **Discussion:** Surprisingly, the above theorem shows that FEDMUON converges to the stationary
 347 point, regardless of how many times we run the Newton-Schulz iteration. The only difference between
 348 the case when we solve the LMO exactly, i.e., Theorem 2, and the case when we solve the LMO
 349 approximately, i.e., Theorem 3, is that Theorem 2 establishes the convergence in the trace norm of
 350 the gradient $\|\nabla f(\mathbf{X})\|_{\text{trace}} (= \|\nabla f(\mathbf{X})\|_1)$,¹ while Theorem 3 establishes the convergence in the
 351 Schatten p -norm $\|\nabla f(\mathbf{X})\|_p$. We recover the convergence rate of Theorem 2 by setting $T \rightarrow \infty$,
 352 and therefore have $p \rightarrow 1$. Since we have $\|\mathbf{A}\|_q \leq \|\mathbf{A}\|_p$ when $1 \leq p \leq q$, Theorem 3 implies
 353 that FEDMUON can converge faster when we increase the number of Newton-Schulz iterations T .
 354 More specifically, since it holds that $\|\mathbf{A}\|_1 \leq \sqrt{\min\{d_1, d_2\}} \|\mathbf{A}\|_2$, solving the LMO accurately
 355 can improve the convergence rate by up to a factor of $\sqrt{\min\{d_1, d_2\}}$. In our experiments, we will
 356 demonstrate that FEDMUON can train neural networks even if $T = 0$, while FEDMUON can achieve
 357 higher accuracy as T increases (see Section 7.2). These observations are consistent with Theorem 3.

358 The quantity of $(1 - \kappa)^{1.5^T}$ in the definition of p measures how fast the Newton-Schulz iteration
 359 converges. If we consider the worst case, κ could be arbitrarily close to zero, and thus a large T would
 360 be required to sufficiently decrease p . However, the main implication of Theorem 3 is that increasing
 361 T leads to an improved convergence rate. Indeed, our experiments show that even increasing T from
 362 0 to 1 dramatically improves accuracy (see Section 7.2).

363 **Comparison with Existing Analysis with Inexact LMO:** There are many papers that analyzed
 364 the convergence rate of Muon, while most of them assumed that the LMO is exactly solved (Pethick
 365 et al., 2025; Riabinin et al., 2025; Shen et al., 2025). The only study analyzing the rate with an inexact
 366 LMO is Refael et al. (2025). However, they also assumed that we run Newton-Schulz iterations a
 367 certain number of times (see Lemma 3.3 and Remark 3.6 in (Refael et al., 2025)). Compared with
 368 these prior analyses, our novel analysis provides a stronger claim that FEDMUON can converge to
 369 the stationary point for any number of the Newton-Schulz iterations $T \geq 0$. Furthermore, it is first
 370 observed by Theorem 3 that the different norms of the gradient are bounded depending on T .

371 ¹When $\|\cdot\|$ is the spectral norm, its dual norm is the trace norm.

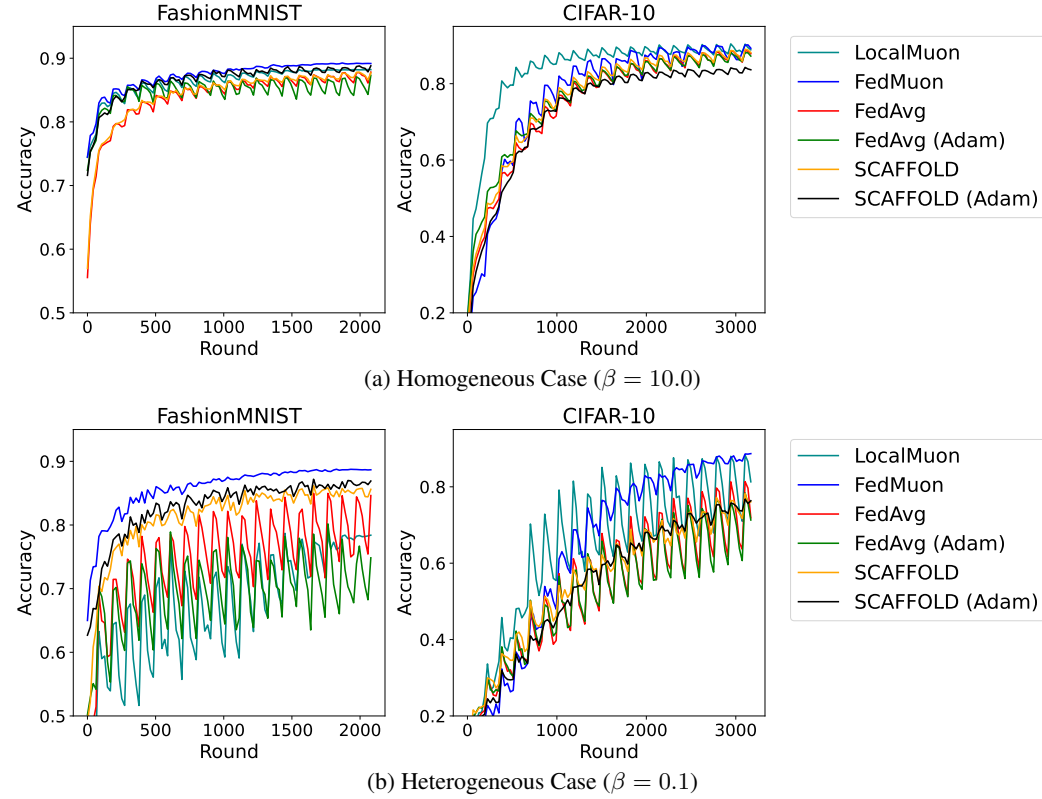


Figure 1: Training curves of various methods. For all settings, FEDMUON can achieve higher test accuracy than other methods.

Proof Sketch: In the following, we provide an intuition for why FEDMUON can converge for any $T \geq 0$. If we solve the LMO exactly, we have

$$\langle \mathbf{G}, \text{lmo}_{\text{muon}}(\mathbf{G}) \rangle = -\|\mathbf{G}\|_{\text{trace}}, \quad \|\text{lmo}_{\text{muon}}(\mathbf{G})\|_{\text{sp}} \leq 1. \quad (4)$$

The first equality holds from the definition of the dual norm (see Lemma 1), and the second inequality holds since the solution of the LMO satisfies the constraint. Then, the output of the Newton-Schulz iteration satisfies the following (see Lemma 12):

$$-\|\mathbf{G}\|_{\text{trace}} \leq \langle \mathbf{G}, -\mathbf{G}^{(T)} \rangle \leq -\|\mathbf{G}\|_p, \quad \left\| -\mathbf{G}^{(T)} \right\|_{\text{sp}} \leq 1. \quad (5)$$

The above inequality indicates that even if we run the Newton-Schulz iteration only a few times to solve the LMO approximately, the output of the Newton-Schulz iteration is a proper direction to minimize the loss function, and FEDMUON can converge to the stationary point. For instance, when $T = 0$, the output of Newton-Schulz iteration is $-\frac{\mathbf{G}}{\|\mathbf{G}\|_F}$, which corresponds to the normalized gradient, and it is natural that FEDMUON can converge to the stationary point when $T = 0$. Then, if we run the Newton-Schulz iteration T times, the output of the Newton-Schulz iteration comes close to the exact solution of LMO and remains a proper direction to minimize the loss function. Thanks to this property, FEDMUON can converge to the stationary point for any number of Newton-Schulz iterations T .

7 EXPERIMENT

7.1 FEDERATED LEARNING TASKS

Setup: We used FashionMNIST (Xiao et al., 2017) and CIFAR-10 (Krizhevsky, 2009) as training datasets, and used LeNet (Lecun et al., 1998) for Fashion MNIST and ResNet-18 (He et al., 2016) for CIFAR-10. Following the prior paper (Hsieh et al., 2020), we used Group Normalization (Wu & He,

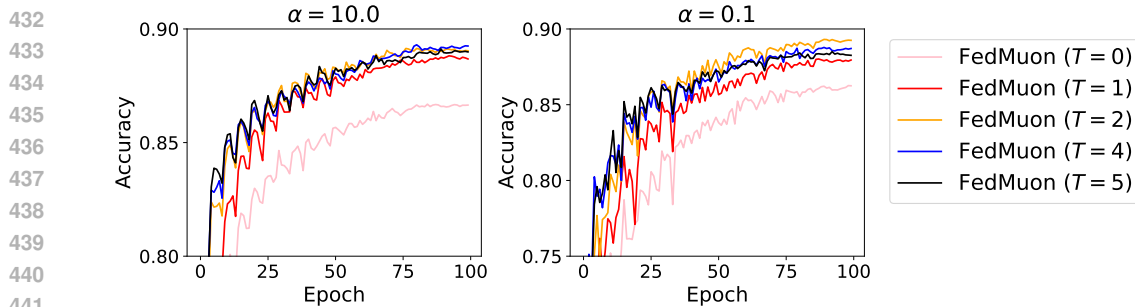


Figure 2: Training curves of FEDMUON with various number of Newton-Schulz iterations. We used FashionMNIST and LeNet.

2018) instead of Batch Normalization (Ioffe & Szegedy, 2015) for ResNet-18. We set the number of clients n to 16 and sampled $S = 8$ clients every round. We set the number of local steps K to 5 and set the number of epochs to 100 and 200 for FashionMNIST and CIFAR-10, respectively. Following the prior paper (Hsu et al., 2019), we distributed the training dataset to clients by using Dirichlet distributions with hyperparameter β . As β approaches zero, each clients come to have a different training dataset. We tuned the stepsize by grid search. See Appendix G for details. The experiments were repeated with two different seed values, and we reported the average.

Comparison Methods: We compared the following methods: (1) FedAvg (McMahan et al., 2017): We used Momentum SGD as the optimizer. (2) FedAvg (Adam): We used Adam as the optimizer of FedAvg. (3) SCAFFOLD (Karimireddy et al., 2020): We used Momentum SGD as the optimizer. (4) SCAFFOLD (Adam): We used Adam as the optimizer of SCAFFOLD. (5) FEDMUON: Our proposed method. Following the suggestion of Liu et al. (2025a), we changed the scale of the stepsize per layer, depending on the dimension.

Results: We show the results in Fig. 1. The results indicate that FEDMUON can perform the best for all settings. By comparing FEDMUON with FedAvg (Adam) and SCAFFOLD (Adam), FEDMUON achieved the highest accuracy, which can demonstrate that Muon is also beneficial in the federated learning setting. By comparing FEDMUON and LOCALMUON, LOCALMUON performed well in the homogeneous setting, but did not match the performance of FEDMUON in the heterogeneous setting. This observation is consistent with the discussion in Section 3, where we show that LOCALMUON does not converge to the stationary point in the heterogeneous setting. These observations were consistent with Theorem 1.

7.2 EFFECT OF INEXACT LMO

Next, we evaluate how the number of Newton-Schulz iterations T affects the performance. Figure 2 shows the training curves of FEDMUON with different T . In the homogeneous setting, the highest accuracy was achieved when $T = 4$, and in the heterogeneous setting, the highest accuracy was achieved when $T = 2$. Thus, we can observe that solving the LMO accurately can improve the performance. Notably, FEDMUON already worked with $T = 0$, but increasing T from 0 to 1 led to a significant improvement in accuracy. These observations were consistent with Theorem 3, which shows that FEDMUON can converge for any T and converge faster as T increases.

8 CONCLUSION

In this paper, we study the federated learning methods with the LMO and propose FEDMUON. We first propose directly plugging the optimization methods with the LMO into FedAvg, which we referred to as LOCALMUON, and show that LOCALMUON cannot converge to the stationary point since the LMO is a biased operator. We then propose FEDMUON to solve this issue and show that FEDMUON can converge to the stationary point. We analyze the convergence rate of FEDMUON and reveal how the approximate solution of the LMO affects the convergence behavior. Notably, we show that FEDMUON can converge for any number of Newton-Schulz iterations, and FEDMUON can converge faster as we solve the LMO more accurately. Throughout the experiments, we demonstrated the effectiveness of FEDMUON and verified our theoretical discovery.

486 REFERENCES
487488 Kwangjun Ahn, Byron Xu, Natalie Abreu, Ying Fan, Gagik Magakyan, Pratyusha Sharma, Zheng
489 Zhan, and John Langford. Dion: Distributed orthonormalized updates. In *arXiv*, 2025.490 Dan Alistarh, Demjan Grubic, Jerry Li, Ryota Tomioka, and Milan Vojnovic. Qsgd: Communication-
491 efficient SGD via gradient quantization and encoding. In *Advances in Neural Information Processing*
492 *Systems*, 2017.493 Shun-ichi Amari. Natural gradient works efficiently in learning. In *Neural Computation*, 1998.494 Noah Amsel, David Persson, Christopher Musco, and Robert M. Gower. The polar express: Optimal
495 matrix sign methods and their application to the muon algorithm. In *arXiv*, 2025.496 Sébastien Bubeck. Convex optimization: Algorithms and complexity. In *Foundations and Trends in*
497 *Machine Learning*, 2015.498 Wenlin Chen, Samuel Horváth, and Peter Richtárik. Optimal client sampling for federated learning.
499 In *Transactions on Machine Learning Research*, 2022.500 Ziheng Cheng, Xinmeng Huang, Pengfei Wu, and Kun Yuan. Momentum benefits non-iid federated
501 learning simply and provably. In *International Conference on Learning Representations*, 2024.502 John B. Conway. A course in functional analysis. In *Springer*. 2019.503 Ashok Cutkosky and Harsh Mehta. Momentum improves normalized SGD. In *International*
504 *Conference on Machine Learning*, 2020.505 George E. Dahl, Frank Schneider, Zachary Nado, Naman Agarwal, Chandramouli Shama Sastry,
506 Philipp Hennig, Sourabh Medapati, Runa Eschenhagen, Priya Kasimbeg, Daniel Suo, Juhan Bae,
507 Justin Gilmer, Abel L. Peirson, Bilal Khan, Rohan Anil, Mike Rabbat, Shankar Krishnan, Daniel
508 Snider, Ehsan Amid, Kongtao Chen, Chris J. Maddison, Rakshith Vasudev, Michal Badura, Ankush
509 Garg, and Peter Mattson. Benchmarking neural network training algorithms. In *arXiv*, 2025.510 Aaron Defazio, Xingyu Alice Yang, Ahmed Khaled, Konstantin Mishchenko, Harsh Mehta, and
511 Ashok Cutkosky. The road less scheduled. In *Advances in Neural Information Processing Systems*,
512 2024.513 John Duchi, Elad Hazan, and Yoram Singer. Adaptive subgradient methods for online learning and
514 stochastic optimization. In *Journal of Machine Learning Research*, 2011.515 Anis Elgabli, Chaouki Ben Issaid, Amrit Singh Bedi, Ketan Rajawat, Mehdi Bennis, and Vaneet
516 Aggarwal. FedNew: A communication-efficient and privacy-preserving Newton-type method for
517 federated learning. In *International Conference on Machine Learning*, 2022.518 M Frank and P Wolfe. An algorithm for quadratic programming. In *Naval Research Logistics*
519 Quarterly, 1956.520 Yuan Gao, Rustem Islamov, and Sebastian U Stich. EControl: Fast distributed optimization with
521 compression and error control. In *International Conference on Learning Representations*, 2024.522 Ekaterina Grishina, Matvey Smirnov, and Maxim Rakhuba. Accelerating newton-schulz iteration for
523 orthogonalization via chebyshev-type polynomials. In *arXiv*, 2025.524 Xinran Gu, Kaixuan Huang, Jingzhao Zhang, and Longbo Huang. Fast federated learning in the
525 presence of arbitrary device unavailability. In *Advances in Neural Information Processing Systems*,
526 2021.527 Vineet Gupta, Tomer Koren, and Yoram Singer. Shampoo: Preconditioned stochastic tensor optimiza-
528 tion. In *International Conference on Machine Learning*, 2018.529 Kaiming He, Xiangyu Zhang, Shaoqing Ren, and Jian Sun. Deep residual learning for image
530 recognition. In *IEEE / CVF Computer Vision and Pattern Recognition Conference*, 2016.

540 Yutong He, Xinmeng Huang, and Kun Yuan. Unbiased compression saves communication in
 541 distributed optimization: When and how much? In *Advances in Neural Information Processing*
 542 *Systems*, 2023.

543

544 Kevin Hsieh, Amar Phanishayee, Onur Mutlu, and Phillip Gibbons. The non-IID data quagmire of
 545 decentralized machine learning. In *International Conference on Machine Learning*, 2020.

546

547 Tzu-Ming Harry Hsu, Hang Qi, and Matthew Brown. Measuring the effects of non-identical data
 548 distribution for federated visual classification. In *arXiv*, 2019.

549

550 Sergey Ioffe and Christian Szegedy. Batch normalization: Accelerating deep network training by
 551 reducing internal covariate shift. In *International Conference on Machine Learning*, 2015.

551

552 Satoki Ishikawa and Ryo Karakida. On the parameterization of second-order optimization effective
 553 towards the infinite width. In *International Conference on Learning Representations*, 2024.

554

555 Rustem Islamov, Mher Safaryan, and Dan Alistarh. AsGrad: A sharp unified analysis of asynchronous-
 556 SGD algorithms. In *International Conference on Artificial Intelligence and Statistics*, 2024.

556

557 Martin Jaggi. Revisiting Frank-Wolfe: Projection-free sparse convex optimization. In *International*
 558 *Conference on Machine Learning*, 2013.

559

560 Xiaowen Jiang, Anton Rodomanov, and Sebastian U. Stich. Stabilized proximal-point methods for
 561 federated optimization. In *Advances in Neural Information Processing Systems*, 2024a.

561

562 Xiaowen Jiang, Anton Rodomanov, and Sebastian U. Stich. Federated optimization with doubly
 563 regularized drift correction. In *International Conference on Machine Learning*, 2024b.

564

565 Keller Jordan, Yuchen Jin, Vlado Boza, You Jiacheng, Franz Cesista, Laker Newhouse, and Jeremy
 566 Bernstein. Muon: An optimizer for hidden layers in neural networks, 2024. URL <https://kellerjordan.github.io/posts/muon/>.

567

568 Peter Kairouz, H. Brendan McMahan, Brendan Avent, Aurélien Bellet, Mehdi Benni, Arjun Nitin
 569 Bhagoji, Kallista Bonawitz, Zachary Charles, Graham Cormode, Rachel Cummings, Rafael G. L.
 570 D’Oliveira, Hubert Eichner, Salim El Rouayheb, David Evans, Josh Gardner, Zachary Garrett,
 571 Adrià Gascón, Badih Ghazi, Phillip B. Gibbons, Marco Gruteser, Zaid Harchaoui, Chaoyang
 572 He, Lie He, Zhouyuan Huo, Ben Hutchinson, Justin Hsu, Martin Jaggi, Tara Javidi, Gauri Joshi,
 573 Mikhail Khodak, Jakub Konecný, Aleksandra Korolova, Farinaz Koushanfar, Sanmi Koyejo,
 574 Tancrède Lepoint, Yang Liu, Prateek Mittal, Mehryar Mohri, Richard Nock, Ayfer Özgür, Rasmus
 575 Pagh, Hang Qi, Daniel Ramage, Ramesh Raskar, Mariana Raykova, Dawn Song, Weikang Song,
 576 Sebastian U. Stich, Ziteng Sun, Ananda Theertha Suresh, Florian Tramèr, Praneeth Vepakomma,
 577 Jianyu Wang, Li Xiong, Zheng Xu, Qiang Yang, Felix X. Yu, Han Yu, and Sen Zhao. Advances
 578 and open problems in federated learning. In *Foundations and Trends in Machine Learning*, 2021.

578

579 Sai Praneeth Karimireddy, Quentin Rebjock, Sebastian Stich, and Martin Jaggi. Error feedback fixes
 580 signs gd and other gradient compression schemes. In *International conference on machine learning*,
 581 2019.

582

583 Sai Praneeth Karimireddy, Satyen Kale, Mehryar Mohri, Sashank Reddi, Sebastian Stich, and
 584 Ananda Theertha Suresh. SCAFFOLD: Stochastic controlled averaging for federated learning. In
 585 *International Conference on Machine Learning*, 2020.

585

586 Sai Praneeth Karimireddy, Martin Jaggi, Satyen Kale, Mehryar Mohri, Sashank J. Reddi, Sebastian U
 587 Stich, and Ananda Theertha Suresh. Breaking the centralized barrier for cross-device federated
 588 learning. In *Advances in Neural Information Processing Systems*, 2021.

589

590 Diederik P. Kingma and Jimmy Ba. Adam: A method for stochastic optimization. In *International*
 591 *Conference on Learning Representations*, 2017.

592

593 Anastasia Koloskova, Nicolas Loizou, Sadra Boreiri, Martin Jaggi, and Sebastian Stich. A unified
 594 theory of decentralized SGD with changing topology and local updates. In *International Conference*
 595 *on Machine Learning*, 2020.

594 Anastasia Koloskova, Sebastian U Stich, and Martin Jaggi. Sharper convergence guarantees for
 595 asynchronous SGD for distributed and federated learning. In *Advances in Neural Information
 596 Processing Systems*, 2022.

597 Dmitry Kovalev. Understanding gradient orthogonalization for deep learning via non-euclidean
 598 trust-region optimization. In *arXiv*, 2025.

600 Alex Krizhevsky. Learning multiple layers of features from tiny images. In *Technical Report*, 2009.

601

602 Y. Lecun, L. Bottou, Y. Bengio, and P. Haffner. Gradient-based learning applied to document
 603 recognition. In *IEEE*, 1998.

604 Tao Lin, Sai Praneeth Karimireddy, Sebastian Stich, and Martin Jaggi. Quasi-global momentum:
 605 Accelerating decentralized deep learning on heterogeneous data. In *International Conference on
 606 Machine Learning*, 2021.

607

608 Jingyuan Liu, Jianlin Su, Xingcheng Yao, Zhejun Jiang, Guokun Lai, Yulun Du, Yidao Qin, Weixin
 609 Xu, Enzhe Lu, Junjie Yan, Yanru Chen, Huabin Zheng, Yibo Liu, Shaowei Liu, Bohong Yin,
 610 Weiran He, Han Zhu, Yuzhi Wang, Jianzhou Wang, Mengnan Dong, Zheng Zhang, Yongsheng
 611 Kang, Hao Zhang, Xinran Xu, Yutao Zhang, Yuxin Wu, Xinyu Zhou, and Zhilin Yang. Muon is
 612 scalable for llm training. In *arXiv*, 2025a.

613 Liming Liu, Zhenghao Xu, Zixuan Zhang, Hao Kang, Zichong Li, Chen Liang, Weizhu Chen, and
 614 Tuo Zhao. Cosmos: A hybrid adaptive optimizer for memory-efficient training of llms. In *arXiv*,
 615 2025b.

616

617 Ilya Loshchilov and Frank Hutter. Decoupled weight decay regularization. In *International Confer-
 618 ence on Learning Representations*, 2019.

619 Chao Ma, Wenbo Gong, Meyer Scetbon, and Edward Meeds. Swan: SGD with normalization and
 620 whitening enables stateless llm training. In *arXiv*, 2025.

621

622 Brendan McMahan, Eider Moore, Daniel Ramage, Seth Hampson, and Blaise Aguera y Arcas.
 623 Communication-Efficient Learning of Deep Networks from Decentralized Data. In *International
 624 Conference on Artificial Intelligence and Statistics*, 2017.

625 Konstantin Mishchenko, Francis Bach, Mathieu Even, and Blake Woodworth. Asynchronous SGD
 626 beats minibatch SGD under arbitrary delays. In *Advances in Neural Information Processing
 627 Systems*, 2022.

628

629 Angelia Nedić, Alex Olshevsky, and Wei Shi. Achieving geometric convergence for distributed
 630 optimization over time-varying graphs. In *SIAM Journal on Optimization*, 2017.

631 Yurii Nesterov. Lectures on convex optimization. In *Springer*, 2018.

632

633 Thomas Pethick, Wanyun Xie, Kimon Antonakopoulos, Zhenyu Zhu, Antonio Silveti-Falls, and
 634 Volkan Cevher. Training deep learning models with norm-constrained LMOs. In *International
 635 Conference on Machine Learning*, 2025.

636

637 Sashank J. Reddi, Zachary Charles, Manzil Zaheer, Zachary Garrett, Keith Rush, Jakub Konečný,
 638 Sanjiv Kumar, and Hugh Brendan McMahan. Adaptive federated optimization. In *International
 639 Conference on Learning Representations*, 2021.

640

641 Yehonathan Refael, Guy Smorodinsky, Tom Tirer, and Ofir Lindenbaum. Sumo: Subspace-aware
 642 moment-orthogonalization for accelerating memory-efficient llm training. In *arXiv*, 2025.

643

644 Artem Riabinin, Egor Shulgin, Kaja Gruntkowska, and Peter Richtárik. Gluon: Making muon &
 645 scion great again! (bridging theory and practice of LMO-based optimizers for LLMs). In *arXiv*,
 2025.

646

647 Anton Rodomanov, Xiaowen Jiang, and Sebastian U Stich. Universality of adagrad stepsizes for
 648 stochastic optimization: Inexact oracle, acceleration and variance reduction. In *Advances in Neural
 649 Information Processing Systems*, 2024.

648 Günther Schulz. Iterative berechung der reziproken matrix. In *Zeitschrift für Angewandte Mathematik*
 649 *und Mechanik*, 1933.

650

651 Andrei Semenov, Matteo Pagliardini, and Martin Jaggi. Benchmarking optimizers for large language
 652 model pretraining. In *arXiv*, 2025.

653 Wei Shen, Ruichuan Huang, Minhui Huang, Cong Shen, and Jiawei Zhang. On the convergence
 654 analysis of muon. In *arXiv*, 2025.

655 Hao-Jun Michael Shi, Tsung-Hsien Lee, Shintaro Iwasaki, Jose Gallego-Posada, Zhiqing Li, Kaushik
 656 Rangadurai, Dheevatsa Mudigere, and Michael Rabbat. A distributed data-parallel pytorch imple-
 657 mentation of the distributed shampoo optimizer for training neural networks at-scale. In *arXiv*,
 658 2023.

659 Sebastian U. Stich. Local SGD converges fast and communicates little. In *arXiv*, 2019.

660

661 Sebastian U Stich, Jean-Baptiste Cordonnier, and Martin Jaggi. Sparsified sgd with memory. In
 662 *Advances in neural information processing systems*, 2018.

663 Tao Sun, Qingsong Wang, Dongsheng Li, and Bao Wang. Momentum ensures convergence of
 664 SIGNSGD under weaker assumptions. In *International Conference on Machine Learning*, 2023.

665

666 Yuki Takezawa, Han Bao, Kenta Niwa, Ryoma Sato, and Makoto Yamada. Momentum tracking:
 667 Momentum acceleration for decentralized deep learning on heterogeneous data. In *Transactions
 668 on Machine Learning Research*, 2023.

669 Hanlin Tang, Shaoduo Gan, Ce Zhang, Tong Zhang, and Ji Liu. Communication compression for
 670 decentralized training. In *Advances in Neural Information Processing Systems*, 2018a.

671 Hanlin Tang, Xiangru Lian, Ming Yan, Ce Zhang, and Ji Liu. d^2 : Decentralized training over
 672 decentralized data. In *International Conference on Machine Learning*, 2018b.

673

674 Benjamin Thérien, Xiaolong Huang, Irina Rish, and Eugene Belilovsky. Muloco: Muon is a practical
 675 inner optimizer for diloco. In *arXiv*, 2025.

676 Thijs Vogels, Sai Praneeth Karimireddy, and Martin Jaggi. PowerSGD: Practical low-rank gradient
 677 compression for distributed optimization. In *Advances in Neural Information Processing Systems*,
 678 2019.

679 Nikhil Vyas, Depen Morwani, Rosie Zhao, Itai Shapira, David Brandfonbrener, Lucas Janson, and
 680 Sham M. Kakade. SOAP: Improving and stabilizing shampoo using adam for language modeling.
 681 In *International Conference on Learning Representations*, 2025.

682

683 Rachel Ward, Xiaoxia Wu, and Leon Bottou. Adagrad stepsizes: Sharp convergence over nonconvex
 684 landscapes. In *Journal of Machine Learning Research*, 2020.

685 Blake Woodworth, Kumar Kshitij Patel, Sebastian Stich, Zhen Dai, Brian Bullins, Brendan McMahan,
 686 Ohad Shamir, and Nathan Srebro. Is local SGD better than minibatch SGD? In *International
 687 Conference on Machine Learning*, 2020.

688 Yuxin Wu and Kaiming He. Group normalization. In *arXiv*, 2018.

689

690 Han Xiao, Kashif Rasul, and Roland Vollgraf. Fashion-mnist: A novel image dataset for benchmark-
 691 ing machine learning algorithms. In *arXiv*, 2017.

692 Shuo Xie and Zhiyuan Li. Implicit bias of adamw: ℓ_∞ -norm constrained optimization. In *Inter-
 693 national Conference on Machine Learning*, 2024.

694 Manzil Zaheer, Sashank Reddi, Devendra Sachan, Satyen Kale, and Sanjiv Kumar. Adaptive methods
 695 for nonconvex optimization. In *Advances in Neural Information Processing Systems*, 2018.

696

697 Jianyi Zhang, Ang Li, Minxue Tang, Jingwei Sun, Xiang Chen, Fan Zhang, Changyou Chen, Yiran
 698 Chen, and Hai Li. Fed-CBS: A heterogeneity-aware client sampling mechanism for federated
 699 learning via class-imbalance reduction. In *International Conference on Machine Learning*, 2023.

700 Juntang Zhuang, Tommy Tang, Yifan Ding, Sekhar Tatikonda, Nicha C. Dvornek, Xenophon Pa-
 701 pademetris, and James S. Duncan. Adabelief optimizer: Adapting stepsizes by the belief in
 observed gradients. In *Advances in Neural Information Processing Systems*, 2020.

702
703 A LLM USAGE704
705 We used LLM for proofreading, and it did not contribute to the content of the paper itself.706
707 B RELATED WORK708
709 **Federated Learning:** The simplest algorithm for federated learning is FedAvg (McMahan et al.,
710 2017; Stich, 2019). The main challenge of federated learning is reducing communication between
711 the central server and clients. Various techniques such as client sampling (Gu et al., 2021; Chen
712 et al., 2022; Zhang et al., 2023), multiple local steps (Woodworth et al., 2020; Koloskova et al., 2020;
713 Jiang et al., 2024a;b), and communication compression (Alistarh et al., 2017; Stich et al., 2018;
714 Karimireddy et al., 2019; Vogels et al., 2019; He et al., 2023; Gao et al., 2024) have been studied to
715 reduce the communication costs. However, FedAvg still requires a huge amount of communication
716 when clients have different training datasets. Many papers proposed federated learning methods
717 that are robust to data heterogeneity (Karimireddy et al., 2020; Jiang et al., 2024a;b). The seminal
718 work is SCAFFOLD (Karimireddy et al., 2020), which can converge regardless of data heterogeneity.
719 Besides these methods, asynchronous methods (Koloskova et al., 2022; Mishchenko et al., 2022;
720 Islamov et al., 2024) and decentralized methods (Nedić et al., 2017; Tang et al., 2018b;a; Koloskova
721 et al., 2020; Takezawa et al., 2023) have been widely studied to further improve the efficiency.722 **Adaptive Optimization Methods:** Using adaptive optimization methods is standard for training
723 neural networks efficiently (Amari, 1998; Ward et al., 2020; Duchi et al., 2011; Kingma & Ba, 2017;
724 Loshchilov & Hutter, 2019; Zaheer et al., 2018; Zhuang et al., 2020; Defazio et al., 2024; Rodomanov
725 et al., 2024). Over the last decade, Adam (Kingma & Ba, 2017) and AdamW (Loshchilov & Hutter,
726 2019) are the most widely used, but recently, Shampoo (Gupta et al., 2018) won the External Tuning
727 Task of AlgoPerf (Dahl et al., 2025) and is attracting considerable attention (Shi et al., 2023; Vyas
728 et al., 2025; Ishikawa & Karakida, 2024). Muon (Liu et al., 2025a) can be regarded as the simplified
729 version of Shampoo, and many papers have demonstrated that Muon can train neural networks faster
730 than Adam, AdamW, and Shampoo (Liu et al., 2025a; Pethick et al., 2025; Amsel et al., 2025; Liu
731 et al., 2025b; Ma et al., 2025; Amsel et al., 2025; Grishina et al., 2025). Using Muon in distributed
732 environments is one of the popular topics (Thérien et al., 2025; Ahn et al., 2025). Specifically, Ahn
733 et al. (2025) proposed a method to solve the LMO in a distributed way, and Thérien et al. (2025)
734 proposed MuLoCo, which extends Muon by allowing clients to perform several steps before averaging
735 the parameters as in LOCALMUON. However, since they consider settings where all clients have the
736 same dataset, their objective differs from ours. As we explained in Section 3, because the LMO is a
737 biased operator, bias correction mechanisms used in FEDMUON are necessary in federated learning,
738 in which clients have different training datasets.739
740
741
742
743
744
745
746
747
748
749
750
751
752
753
754
755

756 C PSEUDO CODE
757758

759 **Algorithm 3** FedAvg (McMahan et al., 2017)

760 1: **Input:** the total number of clients n , the number of sampled clients S , and the number of local
761 steps K .
762 2: **for** $t \in \{0, 1, \dots, T\}$ **do** (at the server)
763 3: sample S clients $\mathcal{S}_r \subset [n]$.
764 4: **for** $i \in \mathcal{S}_r$ **do** (at the clients)
765 5: $\mathbf{X}_i^{(r,0)} \leftarrow \mathbf{X}^{(r)}$.
766 6: **for** $k = 0, 1, \dots, K - 1$ **do**
767 7: $\mathbf{X}_i^{(r,k+1)} \leftarrow \mathbf{X}_i^{(r,k)} - \eta \nabla F_i(\mathbf{X}_i^{(r,k)}; \xi_i^{(r,k)})$.
768 8: **end for**
769 9: **end for** (end clients, back to the server)
770 10: $\mathbf{X}^{(r+1)} \leftarrow \frac{n-S}{n} \mathbf{X}^{(r)} + \frac{1}{n} \sum_{i \in \mathcal{S}_r} \mathbf{X}_i^{(r,K)}$.
771 11: **end for**

772

773 **Algorithm 4** LocalMuon

774 1: **Input:** the total number of clients n , the number of sampled clients S , and the number of local
775 steps K .
776 2: **for** $r \in \{0, 1, \dots, R - 1\}$ **do** (at the server)
777 3: sample S clients $\mathcal{S}_r \subset [n]$.
778 4: **for** $i \in \mathcal{S}_r$ **do** (at the clients)
779 5: $\mathbf{X}_i^{(r,0)} \leftarrow \mathbf{X}^{(r)}$ and $\mathbf{M}_i^{(r,0)} \leftarrow \mathbf{M}_i^{(r-1,K)}$
780 6: **for** $k = 0, 1, \dots, K - 1$ **do**
781 7: $\mathbf{M}_i^{(r,k+1)} \leftarrow (1 - \alpha) \mathbf{M}_i^{(r,k)} + \alpha \nabla F_i(\mathbf{X}_i^{(r,k)}; \xi_i^{(r,k)})$.
782 8: $\mathbf{X}_i^{(r,k+1)} \leftarrow \mathbf{X}_i^{(r,k)} + \eta \text{lmo}(\mathbf{M}_i^{(r,k+1)})$.
783 9: **end for**
784 10: $\mathbf{C}_i^{(r+1)} \leftarrow \mathbf{M}_i^{(r,K)}$
785 11: **end for**
786 12: **for** $i \in [n] \setminus \mathcal{S}_r$ **do**
787 13: $\mathbf{M}_i^{(r,K)} \leftarrow \mathbf{M}_i^{(r-1,K)}$.
788 14: **end for** (end clients, back to the server)
789 15: $\mathbf{X}^{(r+1)} \leftarrow \frac{n-S}{n} \mathbf{X}^{(r)} + \frac{1}{n} \sum_{i \in \mathcal{S}_r} \mathbf{X}_i^{(r,K)}$.
790 16: **end for**

792
793
794
795
796
797
798
799
800
801
802
803
804
805
806
807
808
809

810 D PROOF OF THEOREM 1
811812 *Proof.* We consider the setting where $n = 2$, $d = 1$, and the norm is the Euclidean norm. In this case,
813 we have

814
815
$$\text{lmo}(x) = \frac{x}{|x|}.$$

816

817 Then, we consider the case where f_1 and f_2 are defined as follows:

818
819
$$f_1(x) := \frac{x^2}{2},$$

820
821
$$f_2(x) := \frac{(x+a)^2}{2}.$$

822

823 When $M_i^{(0)} = 0$ and $\mathbf{X}^{(0)} = -\frac{a}{4}$, we have

824
825
$$M_1^{(1)} = -\frac{\alpha a}{4},$$

826
827
$$M_2^{(1)} = \frac{3\alpha a}{4},$$

828
829
$$\text{lmo}(M_1^{(1)}) + \text{lmo}(M_2^{(1)}) = 0,$$

830 where we use $\alpha \in (0, 1]$.
831832 Thus, the parameter does not change, i.e., $\mathbf{X}^{(1)} = \mathbf{X}^{(0)}$. For the next round, we have

833
834
$$M_1^{(2)} = -\frac{a}{4}(\alpha + \alpha(1 - \alpha)),$$

835
836
$$M_2^{(2)} = \frac{3a}{4}(\alpha + \alpha(1 - \alpha)).$$

837 Then, since it holds the following as in the first round:
838

839
$$\text{lmo}(M_1^{(2)}) + \text{lmo}(M_2^{(2)}) = 0.$$

840

841 The parameter does not change. Due to the above discussion, the parameter does not change for any
842 r . Now, we have

843
844
$$\|\nabla f(\mathbf{X}^{(r)})\|^2 = \frac{a^2}{16}. \tag{6}$$

845

846 Then, using $\frac{1}{2} \sum_{i=1}^2 \|\nabla f(\mathbf{X}^*)\|^2 = \frac{5a^2}{16}$, we obtain the desired result. \square
847
848
849
850
851
852
853
854
855
856
857
858
859
860
861
862
863

864 E PROOF OF THEOREM 2
865866 E.1 NOTATION
867868 In this section, we use the following notation.
869

870
871
$$\mathbf{X}^{(r,k)} = \frac{n-S}{n} \mathbf{X}^{(r)} + \frac{1}{n} \sum_{i \in \mathcal{S}_r} \mathbf{X}_i^{(r,k)}, \quad (7)$$

872

873
874
$$\mathbf{G}_i^{(r,k+1)} = \mathbf{M}_i^{(r,k+1)} - \mathbf{C}_i^{(r)} + \mathbf{C}^{(r)}, \quad (8)$$

875

876
$$\mathbf{D}_i^{(r,k+1)} = \text{lmo}(\mathbf{G}_i^{(r,k+1)}). \quad (9)$$

877 E.2 USEFUL LEMMA
878879 **Lemma 1.** For any $\mathbf{X} \in \mathcal{X}$, we have
880

881
$$\langle \mathbf{X}, \text{lmo}(\mathbf{X}) \rangle = -\|\mathbf{X}\|_{\star}.$$

882

883 *Proof.* From the definition of $\text{lmo}(\cdot)$, we have
884

885
$$\begin{aligned} \langle \mathbf{X}, \text{lmo}(\mathbf{X}) \rangle &= \min_{\mathbf{Y} \in \{\mathbf{Y} \in \mathcal{X} \mid \|\mathbf{Y}\| \leq 1\}} \langle \mathbf{X}, \mathbf{Y} \rangle \\ &= -\max_{\mathbf{Y} \in \{\mathbf{Y} \in \mathcal{X} \mid \|\mathbf{Y}\| \leq 1\}} \langle -\mathbf{X}, \mathbf{Y} \rangle \\ &= -\| -\mathbf{X} \|_{\star} \\ &= -\| \mathbf{X} \|_{\star}. \end{aligned}$$

886

□

893 **Lemma 2.** For any $k \geq 0, R \geq 0$ and $\alpha \in (0, 1]$, we have
894

895
$$\sum_{r=0}^R k(1-\alpha)^{kr} \leq \frac{1}{\alpha} + k.$$

896

□

897 *Proof.* We have
898

899
$$\sum_{r=0}^R k(1-\alpha)^{kr} \leq \frac{k}{1-(1-\alpha)^k}.$$

900

901 Then, using $(1-\alpha)^k \leq e^{-\alpha k} \leq \frac{1}{1+\alpha k}$, we obtain the desired result.
902

□

903 **Lemma 3.** For any $\mathbf{A}, \mathbf{B} \in \mathcal{X}$, we have
904

905
$$\langle \mathbf{A}, \mathbf{B} \rangle \leq \|\mathbf{A}\| \|\mathbf{B}\|_{\star}.$$

906

907 *Proof.* We have
908

909
$$\langle \mathbf{A}, \mathbf{B} \rangle = \|\mathbf{A}\| \left\langle \frac{\mathbf{A}}{\|\mathbf{A}\|}, \mathbf{B} \right\rangle \leq \|\mathbf{A}\| \|\mathbf{B}\|_{\star}.$$

910

□

911 **Lemma 4.** Suppose that Assumption 1 holds. Then, it holds that for any $\mathbf{X}, \mathbf{Y} \in \mathcal{X}$,
912

913
$$f_i(\mathbf{X}) \leq f_i(\mathbf{Y}) + \langle \nabla f_i(\mathbf{Y}), \mathbf{X} - \mathbf{Y} \rangle + \frac{L}{2} \|\mathbf{X} - \mathbf{Y}\|. \quad (10)$$

914

918 *Proof.* Using the Fundamental Theorem of Calculus, we have
919

$$\begin{aligned}
920 \quad f(\mathbf{X}) &= f(\mathbf{Y}) + \int_{t=0}^1 \langle \nabla f(\mathbf{Y} + t(\mathbf{X} - \mathbf{Y})), \mathbf{X} - \mathbf{Y} \rangle dt \\
921 \\
922 &= f(\mathbf{Y}) + \langle \nabla f(\mathbf{Y}), \mathbf{Y} - \mathbf{X} \rangle + \int_{t=0}^1 \langle \nabla f(\mathbf{Y} + t(\mathbf{X} - \mathbf{Y})) - \nabla f(\mathbf{Y}), \mathbf{X} - \mathbf{Y} \rangle dt \\
923 \\
924 &\leq f(\mathbf{Y}) + \langle \nabla f(\mathbf{Y}), \mathbf{Y} - \mathbf{X} \rangle + \int_{t=0}^1 \|\nabla f(\mathbf{Y} + t(\mathbf{X} - \mathbf{Y})) - \nabla f(\mathbf{Y})\|_* \|\mathbf{X} - \mathbf{Y}\| dt \\
925 \\
926 &\leq f(\mathbf{Y}) + \langle \nabla f(\mathbf{Y}), \mathbf{Y} - \mathbf{X} \rangle + \int_{t=0}^1 Lt \|\mathbf{X} - \mathbf{Y}\|^2 dt \\
927 \\
928 &= f(\mathbf{Y}) + \langle \nabla f(\mathbf{Y}), \mathbf{Y} - \mathbf{X} \rangle + \frac{L}{2} \|\mathbf{X} - \mathbf{Y}\|^2,
\end{aligned}$$

929 where we use Lemma 3 and Assumption 1 for the first and second inequalities, respectively. \square
930

933 E.3 MAIN PROOF

935 **Lemma 5.** Suppose that both $r = r'$ and $k \geq k'$ hold, or $r > r'$ holds. Then, we have
936

$$937 \quad \|\mathbf{X}^{(r,k)} - \mathbf{X}^{(r',k')}\| \leq \frac{\eta S}{n} ((r - r')K + k - k')$$

939 *Proof.* From the update rule of $\mathbf{X}^{(r,k)}$ and $\mathbf{X}^{(r',k')}$, we have
940

$$\begin{aligned}
941 \quad \mathbf{X}^{(r,k)} &= \frac{n - S}{n} \mathbf{X}^{(r)} + \frac{1}{n} \sum_{i \in \mathcal{S}_r} \mathbf{X}_i^{(r,k)} \\
942 \\
943 &= \mathbf{X}^{(r)} + \frac{\eta}{n} \sum_{i \in \mathcal{S}_r} \sum_{k''=1}^k \mathbf{D}_i^{(r,k'')} \\
944 \\
945 &= \mathbf{X}^{(r')} + \frac{\eta}{n} \sum_{i \in \mathcal{S}_r} \sum_{k''=1}^k \mathbf{D}_i^{(r,k'')} + \frac{\eta}{n} \sum_{r''=r'+1}^{r-1} \sum_{i \in \mathcal{S}_{r''}} \sum_{k''=1}^K \mathbf{D}_i^{(r'',k'')}, \\
946 \\
947 \quad \mathbf{X}^{(r',k')} &= \mathbf{X}^{(r')} + \frac{\eta}{n} \sum_{i \in \mathcal{S}_{r'}} \sum_{k''=1}^{k'} \mathbf{D}_i^{(r',k'')}.
\end{aligned}$$

952 Thus, we have
953

$$\begin{aligned}
954 \quad \|\mathbf{X}^{(r,k)} - \mathbf{X}^{(r',k')}\| &= \left\| \frac{\eta}{n} \sum_{i \in \mathcal{S}_r} \sum_{k''=1}^k \mathbf{D}_i^{(r,k'')} + \frac{\eta}{n} \sum_{r''=r'+1}^{r-1} \sum_{i \in \mathcal{S}_{r''}} \sum_{k''=1}^K \mathbf{D}_i^{(r'',k'')} + \frac{\eta}{n} \sum_{i \in \mathcal{S}_{r'}} \sum_{k''=k'+1}^K \mathbf{D}_i^{(r',k'')} \right\| \\
955 \\
956 &\leq \frac{\eta S}{n} ((r - r')K + k - k'),
\end{aligned}$$

959 where we use $\|\mathbf{D}_i^{(r,k)}\| = 1$ for any r and k . \square
960

961 **Lemma 6.** Suppose that both $r = r'$ and $k \geq k'$ hold, or $r > r'$ holds. Then, we have
962

$$963 \quad \|\mathbf{X}_i^{(r,k)} - \mathbf{X}_i^{(r',k')}\| \leq (r - r' + 2)K\eta.$$

964 *Proof.* We have
965

$$\begin{aligned}
966 \quad \|\mathbf{X}_i^{(r,k)} - \mathbf{X}_i^{(r',k')}\| &\leq \|\mathbf{X}_i^{(r,k)} - \mathbf{X}_i^{(r,0)}\| + \|\mathbf{X}_i^{(r,0)} - \mathbf{X}_i^{(r',0)}\| + \|\mathbf{X}_i^{(r',k')} - \mathbf{X}_i^{(r',0)}\| \\
967 \\
968 &= \|\mathbf{X}_i^{(r,k)} - \mathbf{X}_i^{(r,0)}\| + \|\mathbf{X}^{(r,0)} - \mathbf{X}^{(r',0)}\| + \|\mathbf{X}_i^{(r',k')} - \mathbf{X}_i^{(r',0)}\| \\
969 \\
970 &\leq \eta(k + k') + \|\mathbf{X}^{(r,0)} - \mathbf{X}^{(r',0)}\|.
\end{aligned}$$

971 Using Lemma 5, we obtain the desired result. \square

972 **Lemma 7.** Suppose that Assumptions 1 and 2 hold. Then, when $r \geq 1$, we have
 973

$$\begin{aligned}
 974 \mathbb{E}f(\mathbf{X}^{(r,k+1)}) &\leq \mathbb{E}f(\mathbf{X}^{(r,k)}) - \frac{\eta S}{n} \left\| \nabla f(\mathbf{X}^{(r,k)}) \right\|_* + 2LK \left(\frac{S}{n} \right)^2 \eta^2 \\
 975 &\quad + 2 \left(\frac{S}{n} \right) \eta \mathbb{E} \left\| \nabla f(\mathbf{X}^{(r-1,K-1)}) - \mathbf{C}^{(r)} \right\|_* + \frac{2\eta}{n} \mathbb{E} \sum_{i \in \mathcal{S}_r} \left\| \mathbf{M}_i^{(r,k+1)} - \mathbf{C}_i^{(r)} \right\|_* + \frac{L}{2} \left(\frac{S}{n} \right) \eta^2. \\
 976 \\
 977 \\
 978
 \end{aligned}$$

979 When $r = 0$, we have
 980

$$\begin{aligned}
 981 \mathbb{E}f(\mathbf{X}^{(0,k+1)}) &\leq \mathbb{E}f(\mathbf{X}^{(0,k)}) - \frac{\eta S}{n} \left\| \nabla f(\mathbf{X}^{(0,k)}) \right\|_* + 2LK \left(\frac{S}{n} \right)^2 \eta^2 \\
 982 &\quad + \frac{2\eta}{n} \mathbb{E} \sum_{i \in \mathcal{S}_0} \left\| \mathbf{M}_i^{(0,k+1)} - \mathbf{C}_i^{(0)} \right\|_* + \frac{L}{2} \left(\frac{S}{n} \right) \eta^2 + 2 \left(\frac{S}{n} \right) \rho \sigma_0 \eta. \\
 983 \\
 984 \\
 985 \\
 986 \\
 987
 \end{aligned}$$

988 *Proof.* We have
 989

$$\begin{aligned}
 990 \mathbb{E}_{r,k} f(\mathbf{X}^{(r,k+1)}) &= \mathbb{E}_{r,k} f \left(\mathbf{X}^{(r,k)} + \frac{\eta}{n} \sum_{i \in \mathcal{S}_r} \mathbf{D}_i^{(r,k)} \right) \\
 991 &\leq f(\mathbf{X}^{(r,k)}) + \frac{\eta}{n} \mathbb{E}_{r,k} \sum_{i \in \mathcal{S}_r} \left\langle \nabla f(\mathbf{X}^{(r,k)}), \mathbf{D}_i^{(r,k)} \right\rangle + \frac{L\eta^2}{2n} \mathbb{E}_{r,k} \sum_{i \in \mathcal{S}_r} \left\| \mathbf{D}_i^{(r,k+1)} \right\|^2 \\
 992 &\leq f(\mathbf{X}^{(r,k)}) + \frac{\eta}{n} \mathbb{E}_{r,k} \sum_{i \in \mathcal{S}_r} \left\langle \nabla f(\mathbf{X}^{(r,k)}) - \mathbf{G}_i^{(r,k+1)}, \mathbf{D}_i^{(r,k+1)} \right\rangle + \frac{\eta}{n} \mathbb{E}_{r,k} \sum_{i \in \mathcal{S}_r} \left\langle \mathbf{G}_i^{(r,k+1)}, \mathbf{D}_i^{(r,k+1)} \right\rangle + \frac{LS\eta^2}{2n} \\
 993 &\leq f(\mathbf{X}^{(r,k)}) + \frac{\eta}{n} \mathbb{E}_{r,k} \sum_{i \in \mathcal{S}_r} \left\| \nabla f(\mathbf{X}^{(r,k)}) - \mathbf{G}_i^{(r,k+1)} \right\|_* + \frac{\eta}{n} \mathbb{E}_{r,k} \underbrace{\sum_{i \in \mathcal{S}_r} \left\langle \mathbf{G}_i^{(r,k+1)}, \mathbf{D}_i^{(r,k+1)} \right\rangle}_{\mathcal{T}_1} + \frac{LS\eta^2}{2n}, \\
 994 \\
 995 \\
 996 \\
 997 \\
 998 \\
 999 \\
 1000 \\
 1001 \\
 1002 \\
 1003
 \end{aligned}$$

1004 where we use Lemma 4, $\left\| \mathbf{D}_i^{(r,k+1)} \right\| \leq 1$, and the Cauchy-Schwarz inequality in the first, second,
 1005 and third inequalities, and \mathbf{G}_i and \mathbf{D}_i are defined in Appendix E.1. Using Lemma 1 and the triangle
 1006 inequality, we have
 1007

$$\mathcal{T}_1 = - \left\| \mathbf{G}_i^{(r,k+1)} \right\|_* \leq - \left\| \nabla f(\mathbf{X}^{(r,k)}) \right\|_* + \left\| \nabla f(\mathbf{X}^{(r,k)}) - \mathbf{G}_i^{(r,k+1)} \right\|_*.$$

1008 Then, it holds
 1009

$$\mathbb{E}_{r,k} f(\mathbf{X}^{(r,k+1)}) \leq f(\bar{\mathbf{X}}^{(r,k)}) - \frac{\eta S}{n} \left\| \nabla f(\mathbf{X}^{(r,k)}) \right\|_* + \frac{2\eta}{n} \mathbb{E}_{r,k} \underbrace{\sum_{i \in \mathcal{S}_r} \left\| \nabla f(\mathbf{X}^{(r,k)}) - \mathbf{G}_i^{(r,k+1)} \right\|_*}_{\mathcal{T}_2} + \frac{LS\eta^2}{2n}.$$

1010 When $r \geq 1$, we have
 1011

$$\begin{aligned}
 1012 \mathcal{T}_2 &= \left\| \nabla f(\mathbf{X}^{(r,k)}) - \mathbf{M}_i^{(r,k+1)} + \mathbf{C}_i^{(r)} - \mathbf{C}^{(r)} \right\|_* \\
 1013 &\leq \left\| \nabla f(\mathbf{X}^{(r,k)}) - \nabla f(\mathbf{X}^{(r-1,K-1)}) \right\|_* + \left\| \nabla f(\mathbf{X}^{(r-1,K-1)}) - \mathbf{C}^{(r)} \right\|_* + \left\| \mathbf{M}_i^{(r,k+1)} - \mathbf{C}_i^{(r)} \right\|_* \\
 1014 &\leq L \left\| \mathbf{X}^{(r,k)} - \mathbf{X}^{(r-1,K-1)} \right\| + \left\| \nabla f(\mathbf{X}^{(r-1,K-1)}) - \mathbf{C}^{(r)} \right\|_* + \left\| \mathbf{M}_i^{(r,k+1)} - \mathbf{C}_i^{(r)} \right\|_* \\
 1015 &\leq \frac{LSK\eta}{n} + \left\| \nabla f(\mathbf{X}^{(r-1,K-1)}) - \mathbf{C}^{(r)} \right\|_* + \left\| \mathbf{M}_i^{(r,k+1)} - \mathbf{C}_i^{(r)} \right\|_*, \\
 1016 \\
 1017 \\
 1018 \\
 1019 \\
 1020 \\
 1021 \\
 1022 \\
 1023 \\
 1024 \\
 1025
 \end{aligned}$$

where we use Lemma 5 in the last inequality.

1026 When $r = 0$, we have

$$\begin{aligned}
 1028 \quad \mathcal{T}_2 &= \left\| \nabla f(\mathbf{X}^{(0,k)}) - \mathbf{M}_i^{(0,k+1)} + \mathbf{C}_i^{(0)} - \mathbf{C}^{(0)} \right\|_* \\
 1029 &\leq \left\| \nabla f(\mathbf{X}^{(0,k)}) - \nabla f(\mathbf{X}^{(0,0)}) \right\|_* + \left\| \nabla f(\mathbf{X}^{(0,0)}) - \mathbf{C}^{(0)} \right\|_* + \left\| \mathbf{M}_i^{(0,k+1)} - \mathbf{C}_i^{(0)} \right\|_* \\
 1030 &\leq L \left\| \mathbf{X}^{(0,k)} - \mathbf{X}^{(0,0)} \right\| + \left\| \nabla f(\mathbf{X}^{(0,0)}) - \mathbf{C}^{(0)} \right\|_* + \left\| \mathbf{M}_i^{(0,k+1)} - \mathbf{C}_i^{(0)} \right\|_* \\
 1031 &\leq \frac{LSK\eta}{n} + \left\| \nabla f(\mathbf{X}^{(0,0)}) - \mathbf{C}^{(0)} \right\|_* + \left\| \mathbf{M}_i^{(0,k+1)} - \mathbf{C}_i^{(0)} \right\|_*
 \end{aligned}$$

1036 Then, using the following inequality:

$$\begin{aligned}
 1038 \quad \mathbb{E} \left\| \nabla f(\mathbf{X}^{(0,0)}) - \mathbf{C}^{(0)} \right\|_* &\leq \frac{\rho}{n} \sum_{i=1}^n \sqrt{\mathbb{E} \left\| \nabla f_i(\mathbf{X}^{(0,0)}) - \mathbf{C}_i^{(0)} \right\|_F^2} \leq \rho\sigma_0,
 \end{aligned}$$

1041 we obtain the desired result. \square

1043 **Lemma 8.** Suppose that Assumptions 1 and 2 hold, $\mathbf{C}_i^{(0)} := \mathbf{M}_i^{(0,0)}$ and $\mathbf{C}^{(0)} := \frac{1}{n} \sum_{i=1}^n \mathbf{C}_i^{(0)}$,

$$\frac{1}{n} \mathbb{E} \sum_{i \in \mathcal{S}_r} \left\| \nabla F_i(\mathbf{X}_i^{(r-1,K-1)}) - \mathbf{M}_i^{(r,0)} \right\|_* \leq \frac{S\rho\sigma}{n} \left(1 - \frac{S\alpha}{n} \right)^{r-1} + \frac{S}{n} \alpha\rho\sqrt{K\sigma^2} + 6LK\eta.$$

1050 *Proof.* Let $c_i(r-1)$ be the number of times that client i has been sampled by round r . We have

$$\mathbf{M}_i^{(r,0)} = (1 - \alpha)^{c_i(r-1)K} \mathbf{M}_i^{(0,0)} + \alpha \sum_{r'=1}^{c_i(r-1)} \sum_{k'=0}^{K-1} (1 - \alpha)^{(c_i(r-1)-r')K+k} \nabla F_i(\mathbf{X}_i^{(r',k')}; \xi_i^{r',k'})$$

1055 To simplify the notation, we denote $r_i(r')$ by the number of rounds that client i is sampled for the
1056 r' -th time. Using this notation, we have

$$\begin{aligned}
 1058 \quad \mathbf{M}_i^{(r,0)} &= (1 - \alpha)^{c_i(r-1)K} \mathbf{M}_i^{(0,0)} + \alpha \sum_{c'=1}^{c_i(r-1)K} (1 - \alpha)^{c_i(r-1)K-c'} \nabla F_i(\mathbf{X}_i^{(r'(\lceil \frac{c'}{K} \rceil), c'-K\lceil \frac{c'}{K} \rceil)}; \xi_i^{(r'(\lceil \frac{c'}{K} \rceil), c'-K\lceil \frac{c'}{K} \rceil)}) \\
 1059 &= (1 - \alpha)^{c_i(r-1)K} \left(\nabla F_i(\mathbf{X}_i^{(0,0)}; \xi_i^{(0,0)}) - \nabla f_i(\mathbf{X}_i^{(0,0)}) \right) \\
 1060 &\quad + \alpha \sum_{c'=1}^{c_i(r-1)K} (1 - \alpha)^{c_i(r-1)K-c'} \left(\nabla F_i(\mathbf{X}_i^{(r'(\lceil \frac{c'}{K} \rceil), c'-K\lceil \frac{c'}{K} \rceil)}; \xi_i^{(r'(\lceil \frac{c'}{K} \rceil), c'-K\lceil \frac{c'}{K} \rceil)}) - \nabla f_i(\mathbf{X}_i^{(r'(\lceil \frac{c'}{K} \rceil), c'-K\lceil \frac{c'}{K} \rceil)}) \right) \\
 1061 &\quad + (1 - \alpha)^{c_i(r-1)K} \nabla f_i(\mathbf{X}_i^{(0,0)}) + \alpha \underbrace{\sum_{c'=1}^{c_i(r-1)K} (1 - \alpha)^{c_i(r-1)K-c'} \nabla f_i(\mathbf{X}_i^{(r'(\lceil \frac{c'}{K} \rceil), c'-L\lceil \frac{c'}{K} \rceil)})}_{\mathcal{T}}.
 \end{aligned}$$

1073 Using $\alpha(1 - \alpha)^m = (1 - \alpha)^m - (1 - \alpha)^{m+1}$, we have

$$\begin{aligned}
 1074 \quad \mathcal{T} &= \nabla f_i(\mathbf{X}_i^{(r_i(c_i(r-1)), K-1)}) \\
 1075 &\quad + \sum_{c'=1}^{c_i(r-1)K-1} (1 - \alpha)^{c_i(r-1)K-c'} \left(\nabla f_i(\mathbf{X}_i^{(r'(\lceil \frac{c'}{K} \rceil), c'-L\lceil \frac{c'}{K} \rceil)}) - \nabla f_i(\mathbf{X}_i^{(r'(\lceil \frac{c'+1}{K} \rceil), c'+1-K\lceil \frac{c'+1}{K} \rceil)}) \right) \\
 1076 &\quad + (1 - \alpha)^{c_i(r-1)K} \left(\nabla f_i(\mathbf{X}_i^{(0,0)}) - \nabla f_i(\mathbf{X}_i^{(r_i(1), 0)}) \right).
 \end{aligned}$$

1080 Thus, we have
1081
1082 $\mathbb{E} \left\| \mathbf{M}_i^{(r,0)} - \nabla f_i(\mathbf{X}_i^{(r-1,K-1)}) \right\|_{\star}$
1083 $\leq \mathbb{E}(1-\alpha)^{c_i(r-1)K} \rho \sigma$
1084
1085 $+ \alpha \mathbb{E} \left\| \sum_{c'=1}^{c_i(r-1)K} (1-\alpha)^{c_i(r-1)K-c'} \left(\nabla F_i(\mathbf{X}_i^{(r'(\lceil \frac{c'}{K} \rceil), c'-K \lceil \frac{c'}{K} \rceil)}; \xi_i^{(r'(\lceil \frac{c'}{K} \rceil), c'-K \lceil \frac{c'}{K} \rceil)}) - \nabla f_i(\mathbf{X}_i^{(r'(\lceil \frac{c'}{K} \rceil), c'-K \lceil \frac{c'}{K} \rceil)}) \right) \right\|_{\star}$
1086
1087 $+ \mathbb{E} \left\| \nabla f_i(\mathbf{X}_i^{(r_i(c_i(r-1)), K-1)}) - \nabla f_i(\mathbf{X}_i^{(r-1,K-1)}) \right\|_{\star}$
1088
1089 $+ \mathbb{E} \sum_{c'=1}^{c_i(r-1)K-1} (1-\alpha)^{c_i(r-1)K-c'} \left\| \nabla f_i(\mathbf{X}_i^{(r'(\lceil \frac{c'}{K} \rceil), c'-L \lceil \frac{c'}{K} \rceil)}) - \nabla f_i(\mathbf{X}_i^{(r'(\lceil \frac{c'+1}{K} \rceil), c'+1-K \lceil \frac{c'+1}{K} \rceil)}) \right\|_{\star}$
1090
1091 $+ \mathbb{E}(1-\alpha)^{c_i(r-1)K} \left\| \nabla f_i(\mathbf{X}_i^{(0,,0)}) - \nabla f_i(\mathbf{X}_i^{(r_i(1),0)}) \right\|_{\star}$
1092
1093
1094

1095 Using Assumption 1, we have
1096

$$\begin{aligned} & \mathbb{E} \left\| \mathbf{M}_i^{(r,0)} - \nabla f_i(\mathbf{X}_i^{(r-1,K-1)}) \right\|_{\star} \\ & \leq \underbrace{\mathbb{E}(1-\alpha)^{c_i(r-1)K} \rho \sigma}_{\mathcal{T}_1} + \alpha \rho \sqrt{K \sigma^2} \\ & \quad + L \underbrace{\mathbb{E} \sum_{c'=1}^{c_i(r-1)K-1} (1-\alpha)^{c_i(r-1)K-c'} \left\| \mathbf{X}_i^{(r'(\lceil \frac{c'}{K} \rceil), c'-L \lceil \frac{c'}{K} \rceil)} - \mathbf{X}_i^{(r'(\lceil \frac{c'+1}{K} \rceil), c'+1-K \lceil \frac{c'+1}{K} \rceil)} \right\|}_{\mathcal{T}_2} \\ & \quad + L \underbrace{\mathbb{E}(1-\alpha)^{c_i(r-1)K} \left\| \mathbf{X}_i^{(0,,0)} - \mathbf{X}_i^{(r_i(1),0)} \right\|}_{\mathcal{T}_3} \\ & \quad + L \underbrace{\mathbb{E} \left\| \mathbf{X}_i^{(r_i(c_i(r-1)), K-1)} - \mathbf{X}_i^{(r-1,K-1)} \right\|}_{\mathcal{T}_4}. \end{aligned}$$

1112 The quantity of $c_i(r-1)$ is the number of rounds in which client i is sampled, which follows the
1113 binomial distribution.

$$\begin{aligned} \mathcal{T}_1 & \leq \rho \sigma \sum_{c'=0}^{r-1} (1-\alpha)^{Kc'} \left(\frac{S}{n} \right)^{c'} \left(1 - \frac{S}{n} \right)^{r-1-c'} \binom{r-1}{c'} \\ & \leq \rho \sigma \sum_{c'=0}^{r-1} \left((1-\alpha) \frac{S}{n} \right)^{c'} \left(1 - \frac{S}{n} \right)^{r-1-c'} \binom{r-1}{c'} \\ & = \rho \sigma \left(1 - \frac{S\alpha}{n} \right)^{r-1}. \\ \mathcal{T}_2 & \leq \eta \mathbb{E} \sum_{c'=1}^{c_i(r-1)K-1} (1-\alpha)^{c_i(r-1)K-c'} \left(r_i \left(\lceil \frac{c'+1}{K} \rceil \right) - r_i \left(\lceil \frac{c'}{K} \rceil \right) \right) \\ & = \eta \mathbb{E} \sum_{c''=1}^{c_i(r-1)K-1} (1-\alpha)^{c''} \underbrace{\left(r_i \left(\lceil \frac{c'(r-1)K - c'' + 1}{K} \rceil \right) - r_i \left(\lceil \frac{c'(r-1)K - c'' + 1}{K} \rceil \right) \right)}_{\mathcal{T}_5}. \end{aligned}$$

1130 The quantity of \mathcal{T}_5 is the number of rounds from the time cline i was sampled to the next sampling,
1131 which follows a geometric distribution with expectation $\frac{n}{S}$. Thus, we have
1132

$$1133 \mathcal{T}_2 \leq \frac{Kn\eta}{S}$$

1134 Using Lemma 6, we have
 1135

1136 $\mathcal{T}_3 \leq \mathbb{E} \left\| \mathbf{X}_i^{(0,0)} - \mathbf{X}_i^{(r_i(1),0)} \right\|_* = \mathbb{E} \left\| \mathbf{X}^{(0,0)} - \mathbf{X}^{(r_i(1),0)} \right\|_* \leq \frac{\eta S}{n} K \mathbb{E} r_i(1),$
 1138

1139 where we use Lemma 5 in the last inequality. The quantity of $r_i(1)$ is the round in which client i is
 1140 sampled for the first time, which follows a geometric distribution. Thus, we have
 1141

1142 $\mathcal{T}_3 \leq K\eta.$
 1143

1144 Using Lemma 6, we have
 1145

1146 $\mathcal{T}_4 = K\eta (\mathbb{E} (r - 1 - r_i(c_i(r - 1))) + 2).$
 1147

1148 Since the quantity of $r_i(c_i(r - 1))$ is the rounds in which client i is sampled for the last time, we have
 1149

1150 $\mathbb{E} (r - 1 - r_i(c_i(r - 1))) = (r - 1) \left(1 - \frac{S}{n}\right)^r + \sum_{r'=0}^r r' \left(1 - \frac{S}{n}\right)^{r'} \frac{S}{n} \leq \frac{2n}{S}.$
 1151

1152 Thus, it holds that
 1153

1154 $\mathcal{T}_4 \leq \frac{4Kn\eta}{S}.$
 1155

1156 By combining the above inequalities, we obtain the desired result. \square
 1157

1158 **Lemma 9.** Suppose that Assumptions 1 and 2 holds. When $r \geq 1$, it holds that
 1159

1160 $\frac{1}{n} \mathbb{E} \sum_{i \in \mathcal{S}_r} \left\| \mathbf{M}_i^{(r,k+1)} - \mathbf{C}_i^{(r)} \right\|_* \leq 2\alpha \left(\frac{S}{n}\right) \rho \sqrt{K\sigma^2} + 9KL\eta + \left(\frac{S}{n}\right) \rho \sigma_0 \left(1 - \frac{S\alpha}{n}\right)^{r-1},$
 1161

1162 where $\rho := \sup_{\mathbf{X} \in \mathcal{X}} \frac{\|\mathbf{X}\|_*}{\|\mathbf{X}\|_F}$ and $\sigma_0^2 := \frac{1}{n} \sum_{i=1}^n \mathbb{E} \|\nabla f_i(\mathbf{X}_i^{(0)}) - \mathbf{C}_i^{(0)}\|_F^2$.
 1163

1164 Then, when $r = 0$, we have
 1165

1166 $\frac{1}{n} \mathbb{E} \sum_{i \in \mathcal{S}_0} \left\| \mathbf{M}_i^{(0,k+1)} - \mathbf{C}_i^{(0)} \right\|_* \leq \alpha \left(\frac{S}{n}\right) \rho \sqrt{K\sigma^2} + LK\eta + \left(\frac{S}{n}\right) \rho \sigma_0.$
 1167

1168 *Proof.* We have
 1169

1170 $\mathbf{M}_i^{(r,k+1)} = (1 - \alpha)^{k+1} \mathbf{M}_i^{(r,0)} + \alpha \sum_{k'=0}^k (1 - \alpha)^{k-k'} \nabla F_i(\mathbf{X}_i^{(r,k')}; \xi_i^{(r,k')}).$
 1171

1172 Since we have $\mathbf{C}_i^{(r)} = \mathbf{M}_i^{(r,0)}$, we have
 1173

1174 $\mathbb{E} \sum_{i \in \mathcal{S}_r} \left\| \mathbf{M}_i^{(r,k+1)} - \mathbf{C}_i^{(r)} \right\|_* = \alpha \mathbb{E} \sum_{i \in \mathcal{S}_r} \left\| \sum_{k'=0}^k (1 - \alpha)^{k-k'} (\nabla F_i(\mathbf{X}_i^{(r,k')}; \xi_i^{(r,k')}) - \mathbf{M}_i^{(r,0)}) \right\|_*.$
 1175

1188 When $r \geq 1$, we have
 1189

$$\begin{aligned}
 1191 \mathbb{E} \sum_{i \in \mathcal{S}_r} \left\| \mathbf{M}_i^{(r, k+1)} - \mathbf{C}_i^{(r)} \right\|_* &\leq \alpha \mathbb{E} \sum_{i \in \mathcal{S}_r} \left\| \sum_{k'=0}^k (1-\alpha)^{k-k'} \left(\nabla F_i(\mathbf{X}_i^{(r, k')}; \xi_i^{(r, k')}) - \nabla f_i(\mathbf{X}_i^{(r, k')}) \right) \right\|_* \\
 1194 &\quad + \alpha \mathbb{E} \sum_{i \in \mathcal{S}_r} \left\| \sum_{k'=0}^k (1-\alpha)^{k-k'} \left(\nabla f_i(\mathbf{X}_i^{(r, k')}) - \nabla f_i(\mathbf{X}_i^{(r-1, K-1)}) \right) \right\|_* \\
 1197 &\quad + \alpha \mathbb{E} \sum_{i \in \mathcal{S}_r} \left\| \sum_{k'=0}^k (1-\alpha)^{k-k'} \left(\nabla f_i(\mathbf{X}_i^{(r-1, K-1)}) - \mathbf{M}_i^{(r, 0)} \right) \right\|_* \\
 1200 &\leq \alpha \mathbb{E} \sum_{i \in \mathcal{S}_r} \left\| \sum_{k'=0}^k (1-\alpha)^{k-k'} \left(\nabla F_i(\mathbf{X}_i^{(r, k')}; \xi_i^{(r, k')}) - \nabla f_i(\mathbf{X}_i^{(r, k')}) \right) \right\|_* \\
 1203 &\quad + \alpha \mathbb{E} \sum_{i \in \mathcal{S}_r} \left\| \sum_{k'=0}^k (1-\alpha)^{k-k'} \left(\nabla f_i(\mathbf{X}_i^{(r, k')}) - \nabla f_i(\mathbf{X}_i^{(r-1, K-1)}) \right) \right\|_* \\
 1206 &\quad + \mathbb{E} \sum_{i \in \mathcal{S}_r} \left\| \nabla f_i(\mathbf{X}_i^{(r-1, K-1)}) - \mathbf{M}_i^{(r, 0)} \right\|_*.
 \end{aligned}$$

1209
 1210 The first term is bounded from above as follows:
 1211

$$\begin{aligned}
 1213 \mathbb{E} \left\| \sum_{k'=0}^k (1-\alpha)^{k-k'} \left(\nabla F_i(\mathbf{X}_i^{(r, k')}; \xi_i^{(r, k')}) - \nabla f_i(\mathbf{X}_i^{(r, k')}) \right) \right\|_* \\
 1216 &\leq \sqrt{\mathbb{E} \left\| \sum_{k'=0}^k (1-\alpha)^{k-k'} \left(\nabla F_i(\mathbf{X}_i^{(r, k')}; \xi_i^{(r, k')}) - \nabla f_i(\mathbf{X}_i^{(r, k')}) \right) \right\|_*^2} \\
 1220 &= \sqrt{\sum_{k'=0}^k (1-\alpha)^{2(k-k')} \mathbb{E} \left\| \nabla F_i(\mathbf{X}_i^{(r, k')}; \xi_i^{(r, k')}) - \nabla f_i(\mathbf{X}_i^{(r, k')}) \right\|_*^2} \\
 1223 &\leq \rho \sqrt{K \sigma^2},
 \end{aligned}$$

1225 where we used Jensen's inequality in the first inequality. The second term is bounded as follows:
 1226

$$\begin{aligned}
 1228 \left\| \sum_{k'=0}^k (1-\alpha)^{k-k'} \left(\nabla f_i(\mathbf{X}_i^{(r, k')}) - \nabla f_i(\mathbf{X}_i^{(r-1, K-1)}) \right) \right\|_* \\
 1231 &\leq \sum_{k'=0}^k (1-\alpha)^{k-k'} \left\| \nabla f_i(\mathbf{X}_i^{(r, k')}) - \nabla f_i(\mathbf{X}_i^{(r-1, K-1)}) \right\|_* \\
 1234 &\leq L \sum_{k'=0}^k (1-\alpha)^{k-k'} \left\| \mathbf{X}_i^{(r, k')} - \mathbf{X}_i^{(r-1, K-1)} \right\| \\
 1237 &\leq \frac{3LK\eta}{\alpha},
 \end{aligned}$$

1240 where we use Lemma 6 in the last inequality. Then, using Lemma 8, we obtain the desired result
 1241 when $r \geq 1$.

1242 When $r = 0$, we have
 1243

$$\begin{aligned}
 \mathbb{E} \sum_{i \in \mathcal{S}_0} \left\| \mathbf{M}_i^{(0,k+1)} - \mathbf{C}_i^{(0)} \right\|_* &= \alpha \mathbb{E} \sum_{i \in \mathcal{S}_r} \left\| \sum_{k'=0}^k (1-\alpha)^{k-k'} \left(\nabla F_i(\mathbf{X}_i^{(r,k')}; \xi_i^{(r,k')}) - \mathbf{M}_i^{(r,0)} \right) \right\|_* \\
 &\leq \alpha \mathbb{E} \sum_{i \in \mathcal{S}_0} \left\| \sum_{k'=0}^k (1-\alpha)^{k-k'} \left(\nabla F_i(\mathbf{X}_i^{(0,k')}; \xi_i^{(0,k')}) - \nabla f_i(\mathbf{X}_i^{(0,k')}) \right) \right\|_* \\
 &\quad + \alpha \mathbb{E} \sum_{i \in \mathcal{S}_0} \left\| \sum_{k'=0}^k (1-\alpha)^{k-k'} \left(\nabla f_i(\mathbf{X}_i^{(0,k')}) - \nabla f_i(\mathbf{X}_i^{(0,0)}) \right) \right\|_* \\
 &\quad + \alpha \mathbb{E} \sum_{i \in \mathcal{S}_0} \left\| \sum_{k'=0}^k (1-\alpha)^{k-k'} \left(\nabla f_i(\mathbf{X}_i^{(0,0)}) - \mathbf{M}_i^{(0,0)} \right) \right\|_* \\
 &\leq \alpha S \rho \sqrt{K \sigma^2} + L K S \eta + S \rho \mathbb{E} \left\| \nabla f_i(\mathbf{X}_i^{(0,0)}) - \mathbf{C}_i^{(0)} \right\|_F,
 \end{aligned}$$

1258 where we use Assumptions 1 and 2 and $\mathbf{C}_i^{(0)} = \mathbf{M}_i^{(r,0)}$ in the last inequality. Dividing both sides by
 1259 n , we obtain the desired result. \square
 1260

1261
 1262 **Lemma 10.** Suppose that Assumptions 1 and 2 hold, $\mathbf{C}_i^{(0)} := \mathbf{M}_i^{(0,0)}$ and $\mathbf{C}^{(0)} := \frac{1}{n} \sum_{i=1}^n \mathbf{C}_i^{(0)}$,
 1263 we have

$$\mathbb{E} \left\| \nabla f(\mathbf{X}^{(r-1,K-1)}) - \mathbf{C}^{(r)} \right\|_* \leq \frac{\rho S}{n} \sqrt{\frac{\alpha \sigma^2}{S}} + \frac{4nL\eta}{\alpha S} + \frac{6LKn\eta}{S} + \rho \sigma \left(1 - \frac{S\alpha}{n} \right)^{r-1}.$$

1264
 1265 *Proof.* Let $c_i(r-1)$ be the number of times that client i has been sampled by round r . We denote
 1266 $r_i(r')$ by the number of rounds that client i is sampled for the r' -th time. Using this notation, we have
 1267

$$\mathbf{C}^{(r)} = \frac{1}{n} \sum_{i=1}^n \mathbf{M}_i^{(r_i(c_i(r-1)), K)}.$$

1268 Then, we have
 1269

$$\begin{aligned}
 \mathbf{M}_i^{(r-1,K-1)} &= (1-\alpha)^{c_i(r-1)K} \mathbf{M}_i^{(0,0)} + \alpha \sum_{r'=1}^{c_i(r-1)} \sum_{k'=0}^{K-1} (1-\alpha)^{(c_i(r-1)-r')K+k} \nabla F_i(\mathbf{X}_i^{(r',k')}; \xi_i^{r',k'}) \\
 &= (1-\alpha)^{c_i(r-1)K} \left(\mathbf{M}_i^{(0,0)} - \nabla f_i(\mathbf{X}^{(0,0)}) \right) \\
 &\quad + \alpha \sum_{r'=1}^{c_i(r-1)} \sum_{k'=0}^{K-1} (1-\alpha)^{(c_i(r-1)-r')K+k} \underbrace{\left(\nabla F_i(\mathbf{X}_i^{(r',k')}; \xi_i^{r',k'}) - \nabla f_i(\mathbf{X}_i^{(r',k')}) \right)}_{\mathcal{T}_1} \\
 &\quad + (1-\alpha)^{c_i(r-1)K} \nabla f_i(\mathbf{X}^{(0,0)}) + \alpha \sum_{r'=1}^{c_i(r-1)} \sum_{k'=0}^{K-1} (1-\alpha)^{(c_i(r-1)-r')K+k} \underbrace{\nabla f_i(\mathbf{X}_i^{(r',k')})}_{\mathcal{T}_2}.
 \end{aligned}$$

1270 We can rewrite \mathcal{T}_1 and \mathcal{T}_2 as follows:
 1271

$$\mathcal{T}_1 = \alpha \sum_{r'=0}^{r-1} \sum_{k'=1}^K \mathbb{1}_{i \in \mathcal{S}_{r'}} (1-\alpha)^{(c_i(r-1)-r'+1)K-k'} \left(\nabla F_i(\mathbf{X}_i^{(r',k')}; \xi_i^{(r',k')}) - \nabla f_i(\mathbf{X}_i^{(r',k')}) \right).$$

$$\begin{aligned}
1296 \\
1297 \\
1298 \quad \mathcal{T}_2 = (1 - \alpha)^{c_i(r-1)K} \nabla f_i(\mathbf{X}^{(0,0)}) + \alpha \sum_{c'=1}^{c_i(r-1)K} (1 - \alpha)^{c_i(r-1)K - c'} \nabla f_i(\mathbf{X}_i^{(r_i(\lceil \frac{c'}{K} \rceil), c' - K \lceil \frac{c'}{K} \rceil))}) \\
1299 \\
1300 \\
1301 \quad = \nabla f_i(\mathbf{X}_i^{(r_i(c_i(r-1)), K-1)}) \\
1302 \\
1303 \quad + \alpha \sum_{c'=1}^{c_i(r-1)K-1} (1 - \alpha)^{c_i(r-1)K - c'} \left(\nabla f_i(\mathbf{X}_i^{(r_i(\lceil \frac{c'}{K} \rceil), c' - K \lceil \frac{c'}{K} \rceil))}) - \nabla f_i(\mathbf{X}_i^{(r_i(\lceil \frac{c'+1}{K} \rceil), c'+1 - K \lceil \frac{c'+1}{K} \rceil)}) \right) \\
1304 \\
1305 \quad + (1 - \alpha)^{c_i(r-1)K} \left(\nabla f_i(\mathbf{X}^{(0,0)}) - \nabla f_i(\mathbf{X}_i^{(r_i(1), 0)}) \right). \\
1306
\end{aligned}$$

1307 Thus, we have

$$\begin{aligned}
1308 \quad \mathbb{E} \left\| \mathbf{M}^{(r-1, K-1)} - \nabla f(\mathbf{X}^{(r-1, K-1)}) \right\|_* \\
1309 \\
1310 \quad \leq \underbrace{\mathbb{E} (1 - \alpha)^{c_i(r-1)K} \left\| \frac{1}{n} \sum_{i=1}^n \left(\nabla f_i(\mathbf{X}^{(0,0)}; \xi_i^{(0,0)}) - \nabla f_i(\mathbf{X}^{(0,0)}) \right) \right\|_*}_{\mathcal{T}_3} \\
1311 \\
1312 \\
1313 \\
1314 \\
1315 \quad + \underbrace{\alpha \mathbb{E} \left\| \frac{1}{n} \sum_{i=1}^n \sum_{r'=0}^{r-1} \sum_{k'=1}^K \mathbb{1}_{i \in \mathcal{S}_{r'}} (1 - \alpha)^{(c_i(r-1) - r' + 1)K - k'} \left(\nabla F_i(\mathbf{X}_i^{(r', k')}; \xi_i^{(r', k')}) - \nabla f_i(\mathbf{X}_i^{(r', k')}) \right) \right\|_*}_{\mathcal{T}_4} \\
1316 \\
1317 \\
1318 \\
1319 \quad + \underbrace{\frac{1}{n} \sum_{i=1}^n \mathbb{E} \left\| \nabla f_i(\mathbf{X}_i^{(r_i(c_i(r-1)), K-1)}) - \nabla f_i(\mathbf{X}^{(r-1, K-1)}) \right\|_*}_{\mathcal{T}_5} \\
1320 \\
1321 \\
1322 \\
1323 \quad + \underbrace{\frac{1}{n} \sum_{i=1}^n \mathbb{E} \left\| \sum_{c'=1}^{c_i(r-1)K-1} (1 - \alpha)^{c_i(r-1)K - c'} \left(\nabla f_i(\mathbf{X}_i^{(r_i(\lceil \frac{c'}{K} \rceil), c' - K \lceil \frac{c'}{K} \rceil))}) - \nabla f_i(\mathbf{X}_i^{(r_i(\lceil \frac{c'+1}{K} \rceil), c'+1 - K \lceil \frac{c'+1}{K} \rceil)}) \right) \right\|_*}_{\mathcal{T}_6} \\
1324 \\
1325 \\
1326 \\
1327 \quad + \underbrace{\frac{1}{n} \sum_{i=1}^n \mathbb{E} (1 - \alpha)^{c_i(r-1)K} \left\| \nabla f_i(\mathbf{X}^{(0,0)}) - \nabla f_i(\mathbf{X}_i^{(r_i(1), 0)}) \right\|_*}_{\mathcal{T}_7}. \\
1328 \\
1329 \\
1330 \\
1331 \quad \mathcal{T}_3 \leq \mathbb{E} (1 - \alpha)^{c_i(r-1)K} \rho \sigma
\end{aligned}$$

1332 The quantity of $c_i(r-1)$ is the number of rounds in which client i is sampled, which follows the
1333 binomial distribution.

$$\begin{aligned}
1335 \quad \mathcal{T}_3 &\leq \rho \sigma \sum_{c'=0}^{r-1} (1 - \alpha)^{Kc'} \left(\frac{S}{n} \right)^{c'} \left(1 - \frac{S}{n} \right)^{r-1-c'} \binom{r-1}{c'} \\
1336 \\
1337 \\
1338 \quad &\leq \rho \sigma \sum_{c'=0}^{r-1} \left((1 - \alpha) \frac{S}{n} \right)^{c'} \left(1 - \frac{S}{n} \right)^{r-1-c'} \binom{r-1}{c'} \\
1339 \\
1340 \\
1341 \quad &= \rho \sigma \left(1 - \frac{S\alpha}{n} \right)^{r-1} \\
1342 \\
1343
\end{aligned}$$

$$\begin{aligned}
1344 \quad \mathcal{T}_4 &= \frac{1}{n} \mathbb{E} \left\| \sum_{r'=0}^{r-1} \sum_{k'=1}^K \sum_{i \in \mathcal{S}_{r'}} (1 - \alpha)^{(c_i(r-1) - r' + 1)K - k'} \left(\nabla F_i(\mathbf{X}_i^{(r', k')}; \xi_i^{(r', k')}) - \nabla f_i(\mathbf{X}_i^{(r', k')}) \right) \right\|_* \\
1345 \\
1346 \\
1347 \\
1348 \quad &\leq \frac{\rho S}{n} \sqrt{\frac{\sigma^2}{S(1 - (1 - \alpha)^2)}}. \\
1349
\end{aligned}$$

$$\begin{aligned}
1350 \\
1351 \quad \mathcal{T}_5 &= \mathbb{E} \left\| \nabla f_i(\mathbf{X}_i^{(r_i(c_i(r-1)), K-1)}) - \nabla f_i(\mathbf{X}^{(r-1, K-1)}) \right\|_* \\
1352 \\
1353 \quad &\leq L \mathbb{E} \left\| \mathbf{X}_i^{(r_i(c_i(r-1)), K-1)} - \mathbf{X}^{(r-1, K-1)} \right\| \\
1354 \\
1355 \quad &\leq L \mathbb{E} \left\| \mathbf{X}_i^{(r_i(c_i(r-1)), K-1)} - \mathbf{X}_i^{(r_i(c_i(r-1)), 0)} \right\| + L \mathbb{E} \left\| \mathbf{X}^{(r_i(c_i(r-1)), 0)} - \mathbf{X}^{(r-1, K-1)} \right\| \\
1356 \\
1357 \quad &\leq L\eta(K-1) + \frac{LS\eta}{n} \mathbb{E}(((r-1 - r_i(c_i(r-1)))K + K-1)).
\end{aligned}$$

1359 Since the quantity of $r_i(c_i(r-1))$ is the rounds in which client i is sampled for the last time, we have

$$\begin{aligned}
1360 \quad \mathbb{E}(r-1 - r_i(c_i(r-1))) &= (r-1) \left(1 - \frac{S}{n}\right)^r + \sum_{r'=0}^r r' \left(1 - \frac{S}{n}\right)^{r'} \frac{S}{n} \leq \frac{2n}{S}.
\end{aligned}$$

1363 Thus, we have

$$1364 \quad \mathcal{T}_5 \leq 2LK\eta.$$

1365

$$\begin{aligned}
1366 \quad \mathcal{T}_6 &\leq L \mathbb{E} \sum_{c'=1}^{c_i(r-1)K-1} (1-\alpha)^{c_i(r-1)K-c'} \left\| \mathbf{X}_i^{(r_i(\lceil \frac{c'}{K} \rceil), c'-K\lceil \frac{c'}{K} \rceil)} - \mathbf{X}_i^{(r_i(\lceil \frac{c'+1}{K} \rceil), c'+1-K\lceil \frac{c'+1}{K} \rceil)} \right\| \\
1367 \\
1368 \quad &= L \mathbb{E} \sum_{c''=1}^{c_i(r-1)K-2} \sum_{k'=0} (1-\alpha)^{(c_i(r-1)-c'')K-k'} \left\| \mathbf{X}_i^{(r_i(c''), k'+1)} - \mathbf{X}_i^{(r_i(c''), k')} \right\| \\
1369 \\
1370 \quad &\quad + L \mathbb{E} \sum_{c''=1}^{c_i(r-1)} (1-\alpha)^{(c_i(r-1)-c'')K+1} \left\| \mathbf{X}_i^{(r_i(c''), 0)} - \mathbf{X}_i^{(r_i(c''), K-1)} \right\| \\
1371 \\
1372 \quad &\leq + L \mathbb{E} \sum_{c''=1}^{c_i(r-1)K-2} \sum_{k'=0} (1-\alpha)^{(c_i(r-1)-c'')K-k'} \\
1373 \\
1374 \quad &\quad + L\eta \mathbb{E} \sum_{c''=1}^{c_i(r-1)-1} (1-\alpha)^{(c_i(r-1)-c'')K+1} (r_i(c''+1) - r_i(c'') + 2) \\
1375 \\
1376 \quad &\leq \frac{L\eta}{\alpha} + L\eta \mathbb{E} \sum_{c''=1}^{c_i(r-1)-1} (1-\alpha)^{(c_i(r-1)-c'')K+1} (r_i(c''+1) - r_i(c'') + 2).
\end{aligned}$$

1385 The quantity $r_i(c''+1) - r_i(c'')$ follows the geometric distribution, which has the expectation of $\frac{n}{S}$.
1386 Using Lemma 2, we obtain

$$1387 \quad \mathcal{T}_6 \leq \frac{4nL\eta}{\alpha S} + \frac{3nLK\eta}{S}.$$

1389

$$1390 \quad \mathcal{T}_7 \leq L \mathbb{E} (1-\alpha)^{c_i(r-1)K} \left\| \mathbf{X}_i^{(0,0)} - \mathbf{X}_i^{(r_i(1), 0)} \right\| \leq LK\eta \mathbb{E}(r_i(1) + 2),$$

1391

1392 where we used Lemma 6 in the last inequality. The quantity of $r_i(1)$ is the round in which client i is
1393 sampled for the first time, which follows a geometric distribution. Thus, we have

$$1394 \quad \mathcal{T}_7 \leq \frac{3nLK\eta}{S}$$

1396 \square

1397 **Lemma 11.** Suppose that Assumptions 1 and 2 hold, $\mathbf{C}_i^{(0)} := \mathbf{M}_i^{(0,0)}$ and $\mathbf{C}^{(0)} := \frac{1}{n} \sum_{i=1}^n \mathbf{C}_i^{(0)}$,
1398 there exists η and α such that we have

$$\begin{aligned}
1399 \quad \frac{1}{RK} \sum_{r=0}^{R-1} \sum_{k=0}^{K-1} \mathbb{E} \left\| \nabla f(\mathbf{X}^{(r, k)}) \right\|_* &\leq \mathcal{O} \left(\left(\frac{Lr_0\rho^2\sigma^2}{SRK} \right)^{\frac{1}{4}} + \left(\left(\frac{n}{S} \right)^2 \frac{Lr_0\rho\sigma}{R\sqrt{K}} \right)^{\frac{1}{3}} + \left(\frac{Lr_0}{R} \left(\frac{n}{S} \right)^2 \right)^{\frac{1}{2}} + \frac{\rho\sigma_0}{R} \left(\frac{n}{S} \right) \right. \\
1400 \\
1401 \quad &\quad \left. + \rho\sigma_0 \left(\frac{\rho^2\sigma^2KS}{Lr_0Rn^2} \right)^{\frac{1}{2}} + \rho\sigma_0 \left(\left(\frac{n}{S} \right) \frac{\rho^2\sigma^2K^2}{Lr_0R^2} \right)^{\frac{1}{3}} \right)
\end{aligned}$$

1404 *Proof.* Combining Lemmas 7, 9 and 10, when $r \geq 1$, it holds
 1405

$$\begin{aligned} \mathbb{E}f(\mathbf{X}^{(r,k+1)}) &\leq \mathbb{E}f(\mathbf{X}^{(r,k)}) - \eta \left(\frac{S}{n} \right) \left\| \nabla f(\mathbf{X}^{(r,k)}) \right\|_* \\ &\quad + 2\rho\eta \left(\frac{S}{n} \right)^2 \sqrt{\frac{\alpha\sigma^2}{S}} + \frac{8L\eta^2}{\alpha} + 33LK\eta^2 + 4\alpha\rho\eta \left(\frac{S}{n} \right) \sqrt{K\sigma^2} \\ &\quad + 4\rho\eta \left(\frac{S}{n} \right) \sigma_0 \left(1 - \frac{S\alpha}{n} \right)^{r-1}. \end{aligned}$$

1413 When $r = 0$, we have
 1414

$$\begin{aligned} \mathbb{E}f(\mathbf{X}^{(0,k+1)}) &\leq \mathbb{E}f(\mathbf{X}^{(0,k)}) - \frac{\eta S}{n} \left\| \nabla f(\mathbf{X}^{(0,k)}) \right\|_* \\ &\quad + 5LK\eta^2 + 2\alpha\rho\eta \left(\frac{S}{n} \right) \sqrt{K\sigma^2} + 4\rho\eta \left(\frac{S}{n} \right) \sigma_0. \end{aligned}$$

1420 Summing up the above two inequalities, we obtain
 1421

$$\begin{aligned} \frac{1}{RK} \sum_{r=0}^{R-1} \sum_{k=0}^{K-1} \mathbb{E} \left\| \nabla f(\mathbf{X}^{(r,k)}) \right\|_* &\leq \left(\frac{n}{S} \right) \frac{r_0}{RK\eta} + 2\rho \left(\frac{S}{n} \right) \sqrt{\frac{\alpha\sigma^2}{S}} + \frac{8L\eta}{\alpha} \left(\frac{n}{S} \right) + 33LK \left(\frac{n}{S} \right) \eta \\ &\quad + 4\alpha\rho\sqrt{K\sigma^2} + \frac{4\rho\sigma_0}{R} \sum_{r=1}^{R-1} \left(1 - \frac{S\alpha}{n} \right)^{r-1} + \frac{4\rho\sigma_0}{R} \\ &\leq \left(\frac{n}{S} \right) \frac{r_0}{RK\eta} + 2\rho \left(\frac{S}{n} \right) \sqrt{\frac{\alpha\sigma^2}{S}} + \frac{8L\eta}{\alpha} \left(\frac{n}{S} \right) + 33LK \left(\frac{n}{S} \right) \eta \\ &\quad + 4\alpha\rho\sqrt{K\sigma^2} + \frac{8\rho\sigma_0}{R\alpha} \left(\frac{n}{S} \right). \end{aligned}$$

1432 Then, using the following hyperparameters
 1433

$$\begin{aligned} \eta &= \min \left\{ \sqrt{\frac{\alpha r_0}{8LRK}}, \frac{1}{K} \sqrt{\frac{r_0}{33LR}} \right\}, \\ \alpha &= \min \left\{ 1, \left(\frac{n}{S} \right)^2 \sqrt{\frac{8Lr_0S}{RL\rho^2\sigma^2}}, \left(\frac{2Lr_0}{RK^2\rho^2\sigma^2} \left(\frac{n}{S} \right)^2 \right)^{\frac{1}{3}} \right\}, \end{aligned}$$

1439 we obtain the desired result. □
 1440

1441
 1442
 1443
 1444
 1445
 1446
 1447
 1448
 1449
 1450
 1451
 1452
 1453
 1454
 1455
 1456
 1457

1458 **F PROOF OF THEOREM 3**
 1459

1460 **Lemma 12.** Let \mathbf{G} and $-\mathbf{G}^{(T)}$ be the input and output of Algorithm 2 with $a = \frac{15}{8}$, $b = -\frac{5}{4}$, and
 1461 $c = \frac{3}{8}$. For any number of iterations T , we have
 1462

$$1463 \quad \langle \mathbf{G}, -\mathbf{G}^{(T)} \rangle \leq -\|\mathbf{G}\|_p,$$

1464 where p is defined as follows:
 1465

$$1466 \quad p := 1 + \frac{\log \left(1 - (1 - \kappa)^{1.5^T} \right)}{\log \kappa},$$

$$1467 \quad \kappa := \min_i \frac{s_i}{\sqrt{\sum_j s_j^2}} (> 0),$$

$$1468$$

$$1469$$

$$1470$$

1471 and s_i is the non-zero singular value of \mathbf{G} .
 1472

1473 *Proof.* Let the singular value decomposition of \mathbf{G} be $\mathbf{U}\Sigma\mathbf{V}$. Then, the output $-\mathbf{G}^{(T)}$ can be written
 1474 as follows:
 1475

$$-\mathbf{G}^{(T)} = -\mathbf{U}\Sigma^{(T)}\mathbf{V},$$

1477 where $\Sigma^{(T)}$ is defined as follows:
 1478

$$1479 \quad \Sigma_{ii}^{(T)} := \underbrace{\phi \left(\phi \left(\cdots \phi \left(\frac{\Sigma_{ii}}{\|\mathbf{G}\|_F} \right) \right) \right)}_{T \text{times}}.$$

$$1480$$

$$1481$$

1482 Since $\phi(x) > x$, we have
 1483

$$1484 \quad \Sigma_{ii}^{(T)} \geq \frac{\Sigma_{ii}}{\|\mathbf{G}\|_F}.$$

$$1485$$

1486 Using the above inequality, we have
 1487

$$1488 \quad \langle \mathbf{G}, -\mathbf{G}^{(T)} \rangle = -\langle \mathbf{U}\Sigma\mathbf{V}, \mathbf{U}\Sigma^{(T)}\mathbf{V} \rangle$$

$$1489 \quad = -\sum_i \Sigma_{ii} \left(1 - \left(1 - \Sigma_{ii}^{(T)} \right) \right).$$

$$1490$$

1491 When $a = \frac{15}{8}$, $b = -\frac{5}{4}$ and $c = \frac{3}{8}$, we have
 1492

$$1493 \quad 0 \leq 1 - \phi(x) = (1 - x)^2 \left(-\frac{3}{8}x^3 - \frac{3}{4}x^2 + \frac{1}{8}x + 1 \right) \leq (1 - x)^{1.5}$$

$$1494$$

1495 Thus, it holds that
 1496

$$1497 \quad 1 - \Sigma_{ii}^{(T)} \leq \left(1 - \frac{\Sigma_{ii}}{\|\mathbf{G}\|_F} \right)^{1.5^T} \leq \left(1 - \frac{\Sigma_{ii}}{\left(\sum_j \Sigma_{jj}^p \right)^{\frac{1}{p}}} \right)^{1.5^T},$$

$$1498$$

$$1499$$

1500 for any $1 \leq p \leq 2$. Using the above inequality and the definition of p and κ we get
 1501

$$1502 \quad \langle \mathbf{G}, -\mathbf{G}^{(T)} \rangle \leq -\left(\sum_i \Sigma_{ii}^p \right)^{\frac{1}{p}}.$$

$$1503$$

$$1504$$

1505 \square

1506 **Lemma 13.** Suppose that Assumptions 1 and 2 hold. Then, when $r \geq 1$, we have
 1507

$$1508 \quad \mathbb{E}f(\mathbf{X}^{(r,k+1)}) \leq \mathbb{E}f(\mathbf{X}^{(r,k)}) - \frac{\eta S}{n} \left\| \nabla f(\mathbf{X}^{(r,k)}) \right\|_p^2 + 2LK \left(\frac{S}{n} \right)^2 \eta^2$$

$$1509$$

$$1510 \quad + 2 \left(\frac{S}{n} \right) \eta \mathbb{E} \left\| \nabla f(\mathbf{X}^{(r-1,K-1)}) - \mathbf{C}^{(r)} \right\|_{trace} + \frac{2\eta}{n} \mathbb{E} \sum_{i \in \mathcal{S}_r} \left\| \mathbf{M}_i^{(r,k+1)} - \mathbf{C}_i^{(r)} \right\|_{trace} + \frac{L}{2} \left(\frac{S}{n} \right) \eta^2,$$

$$1511$$

1512 where p is defined as follows:
1513

$$1514 \quad p := 1 + \frac{\log(1 - (1 - \kappa)^{1.5^T})}{\log \kappa},$$

$$1515 \quad \kappa := \min_{j,i,r,k} \frac{s_{j,i,r,k}}{\sqrt{\sum_{j'} s_{j',i,r,k}^2}} (> 0),$$

1516
1517
1518
1519
1520 and $\{s_{j,r,k}\}_j$ are non-zero singular values of $\mathbf{M}_i^{(r,k+1)} - \mathbf{C}_i^{(r)} + \mathbf{C}^{(r)}$.
1521

1522 When $r = 0$, we have
1523

$$\mathbb{E}f(\mathbf{X}^{(0,k+1)}) \leq \mathbb{E}f(\mathbf{X}^{(0,k)}) - \frac{\eta S}{n} \|\nabla f(\mathbf{X}^{(0,k)})\|_p + 2LK \left(\frac{S}{n}\right)^2 \eta^2$$

$$+ \frac{2\eta}{n} \mathbb{E} \sum_{i \in \mathcal{S}_0} \|\mathbf{M}_i^{(0,k+1)} - \mathbf{C}_i^{(0)}\|_{\text{trace}} + \frac{L}{2} \left(\frac{S}{n}\right) \eta^2 + 2 \left(\frac{S}{n}\right) \rho \sigma_0 \eta.$$

1524
1525
1526
1527
1528 *Proof.* We have
1529

$$\mathbb{E}_{r,k} f(\mathbf{X}^{(r,k+1)})$$

$$= \mathbb{E}_{r,k} f \left(\mathbf{X}^{(r,k)} + \frac{\eta}{n} \sum_{i \in \mathcal{S}_r} \mathbf{D}_i^{(r,k)} \right)$$

$$\leq f(\mathbf{X}^{(r,k)}) + \frac{\eta}{n} \mathbb{E}_{r,k} \sum_{i \in \mathcal{S}_r} \langle \nabla f(\mathbf{X}^{(r,k)}), \mathbf{D}_i^{(r,k)} \rangle + \frac{L\eta^2}{2n} \mathbb{E}_{r,k} \sum_{i \in \mathcal{S}_r} \|\mathbf{D}_i^{(r,k+1)}\|_{\text{sp}}^2$$

$$\leq f(\mathbf{X}^{(r,k)}) + \frac{\eta}{n} \mathbb{E}_{r,k} \sum_{i \in \mathcal{S}_r} \langle \nabla f(\mathbf{X}^{(r,k)}) - \mathbf{G}_i^{(r,k+1)}, \mathbf{D}_i^{(r,k+1)} \rangle + \frac{\eta}{n} \mathbb{E}_{r,k} \sum_{i \in \mathcal{S}_r} \langle \mathbf{G}_i^{(r,k+1)}, \mathbf{D}_i^{(r,k+1)} \rangle + \frac{LS\eta^2}{2n}$$

$$\leq f(\mathbf{X}^{(r,k)}) + \frac{\eta}{n} \mathbb{E}_{r,k} \sum_{i \in \mathcal{S}_r} \|\nabla f(\mathbf{X}^{(r,k)}) - \mathbf{G}_i^{(r,k+1)}\|_{\text{trace}} + \frac{\eta}{n} \mathbb{E}_{r,k} \sum_{i \in \mathcal{S}_r} \underbrace{\langle \mathbf{G}_i^{(r,k+1)}, \mathbf{D}_i^{(r,k+1)} \rangle}_{\mathcal{T}_1} + \frac{LS\eta^2}{2n},$$

1543 where we use Lemma 4, $\|\mathbf{D}_i^{(r,k+1)}\|_{\text{sp}} \leq 1$, and the Lemma 3 in the first, second, and third inequalities.
1544 Using Lemma 12, the definition of p , and the triangle inequality, we have
1545

$$1546 \quad \mathcal{T}_1 \leq -\|\mathbf{G}_i^{(r,k+1)}\|_p$$

$$1547 \leq -\|\nabla f(\mathbf{X}^{(r,k)})\|_p + \|\nabla f(\mathbf{X}^{(r,k)}) - \mathbf{G}_i^{(r,k+1)}\|_p$$

$$1548 \leq -\|\nabla f(\mathbf{X}^{(r,k)})\|_p + \|\nabla f(\mathbf{X}^{(r,k)}) - \mathbf{G}_i^{(r,k+1)}\|_{\text{trace}},$$

1549 where we use the fact that $p \geq 1$ and $\|\mathbf{A}\|_p \leq \|\mathbf{A}\|_{\text{trace}}$ for any \mathbf{A} . Then, it holds
1550

$$1551 \quad \mathbb{E}_{r,k} f(\mathbf{X}^{(r,k+1)}) \leq f(\bar{\mathbf{X}}^{(r,k)}) - \frac{\eta S}{n} \|\nabla f(\mathbf{X}^{(r,k)})\|_p + \frac{2\eta}{n} \mathbb{E}_{r,k} \sum_{i \in \mathcal{S}_r} \underbrace{\|\nabla f(\mathbf{X}^{(r,k)}) - \mathbf{G}_i^{(r,k+1)}\|_{\text{trace}}}_{\mathcal{T}_2} + \frac{LS\eta^2}{2n}.$$

1552 When $r \geq 1$, we have
1553

$$1554 \quad \mathcal{T}_2 = \|\nabla f(\mathbf{X}^{(r,k)}) - \mathbf{M}_i^{(r,k+1)} + \mathbf{C}_i^{(r)} - \mathbf{C}^{(r)}\|_{\text{trace}}$$

$$1555 \leq \|\nabla f(\mathbf{X}^{(r,k)}) - \nabla f(\mathbf{X}^{(r-1,K-1)})\|_{\text{trace}} + \|\nabla f(\mathbf{X}^{(r-1,K-1)}) - \mathbf{C}^{(r)}\|_{\text{trace}} + \|\mathbf{M}_i^{(r,k+1)} - \mathbf{C}_i^{(r)}\|_{\text{trace}}$$

$$1556 \leq L \|\mathbf{X}^{(r,k)} - \mathbf{X}^{(r-1,K-1)}\|_{\text{sp}} + \|\nabla f(\mathbf{X}^{(r-1,K-1)}) - \mathbf{C}^{(r)}\|_{\text{trace}} + \|\mathbf{M}_i^{(r,k+1)} - \mathbf{C}_i^{(r)}\|_{\text{trace}}$$

$$1557 \leq \frac{LSK\eta}{n} + \|\nabla f(\mathbf{X}^{(r-1,K-1)}) - \mathbf{C}^{(r)}\|_{\text{trace}} + \|\mathbf{M}_i^{(r,k+1)} - \mathbf{C}_i^{(r)}\|_{\text{trace}},$$

1566 where we use Lemma 5 in the last inequality.
 1567

1568 When $r = 0$, we have

$$\begin{aligned}
 1569 \quad \mathcal{T}_2 &= \left\| \nabla f(\mathbf{X}^{(0,k)}) - \mathbf{M}_i^{(0,k+1)} + \mathbf{C}_i^{(0)} - \mathbf{C}^{(0)} \right\|_{\text{trace}} \\
 1570 &\leq \left\| \nabla f(\mathbf{X}^{(0,k)}) - \nabla f(\mathbf{X}^{(0,0)}) \right\|_{\text{trace}} + \left\| \nabla f(\mathbf{X}^{(0,0)}) - \mathbf{C}^{(0)} \right\|_{\text{trace}} + \left\| \mathbf{M}_i^{(0,k+1)} - \mathbf{C}_i^{(0)} \right\|_{\text{trace}} \\
 1571 &\leq L \left\| \mathbf{X}^{(0,k)} - \mathbf{X}^{(0,0)} \right\|_{\text{sp}} + \left\| \nabla f(\mathbf{X}^{(0,0)}) - \mathbf{C}^{(0)} \right\|_{\text{trace}} + \left\| \mathbf{M}_i^{(0,k+1)} - \mathbf{C}_i^{(0)} \right\|_{\text{trace}} \\
 1572 &\leq \frac{LSK\eta}{n} + \left\| \nabla f(\mathbf{X}^{(0,0)}) - \mathbf{C}^{(0)} \right\|_{\text{trace}} + \left\| \mathbf{M}_i^{(0,k+1)} - \mathbf{C}_i^{(0)} \right\|_{\text{trace}}.
 \end{aligned}$$

1573 Then, using the following inequality:
 1574

$$\mathbb{E} \left\| \nabla f(\mathbf{X}^{(0,0)}) - \mathbf{C}^{(0)} \right\|_* \leq \frac{\rho}{n} \sum_{i=1}^n \sqrt{\mathbb{E} \left\| \nabla f_i(\mathbf{X}^{(0,0)}) - \mathbf{C}_i^{(0)} \right\|_F^2} \leq \rho\sigma_0,$$

1575 we obtain the desired result. \square
 1576

1577 **Lemma 14.** Suppose that Assumptions 1 and 2 hold, $\mathbf{C}_i^{(0)} := \mathbf{M}_i^{(0,0)}$ and $\mathbf{C}^{(0)} := \frac{1}{n} \sum_{i=1}^n \mathbf{C}_i^{(0)}$,
 1578 there exists η and α such that we have

$$\begin{aligned}
 1579 \quad \frac{1}{RK} \sum_{r=0}^{R-1} \sum_{k=0}^{K-1} \mathbb{E} \left\| \nabla f(\mathbf{X}^{(r,k)}) \right\|_p &\leq \mathcal{O} \left(\left(\frac{Lr_0\rho^2\sigma^2}{SRK} \right)^{\frac{1}{4}} + \left(\left(\frac{n}{S} \right)^2 \frac{Lr_0\rho\sigma}{R\sqrt{K}} \right)^{\frac{1}{3}} + \left(\frac{Lr_0}{R} \left(\frac{n}{S} \right)^2 \right)^{\frac{1}{2}} + \frac{\rho\sigma_0}{R} \left(\frac{n}{S} \right) \right. \\
 1580 &\quad \left. + \rho\sigma_0 \left(\frac{\rho^2\sigma^2KS}{Lr_0Rn^2} \right)^{\frac{1}{2}} + \rho\sigma_0 \left(\left(\frac{n}{S} \right) \frac{\rho^2\sigma^2K^2}{Lr_0R^2} \right)^{\frac{1}{3}} \right),
 \end{aligned}$$

1581 Then, p is defined as follows:
 1582

$$\begin{aligned}
 1583 \quad p &:= 1 + \frac{\log \left(1 - (1 - \kappa)^{1.5^T} \right)}{\log \kappa}, \\
 1584 \quad \kappa &:= \min_{j,i,r,k} \frac{s_{j,i,r,k}}{\sqrt{\sum_{j'} s_{j',i,r,k}^2}} (> 0),
 \end{aligned}$$

1585 where $\{s_{j,i,r,k}\}_j$ are non-zero singular values of $\mathbf{M}_i^{(r,k+1)} - \mathbf{C}_i^{(r)} + \mathbf{C}^{(r)}$.
 1586

1587 *Proof.* Even if we solve the LMO approximately, the statements of Lemmas 9 and 10 hold. Thus,
 1588 combining Lemmas 9, 10 and 13 and tuning the hyperparameters as in Lemma 11, we obtain the
 1589 desired result. \square
 1590

1591
 1592
 1593
 1594
 1595
 1596
 1597
 1598
 1599
 1600
 1601
 1602
 1603
 1604
 1605
 1606
 1607
 1608
 1609
 1610
 1611
 1612
 1613
 1614
 1615
 1616
 1617
 1618
 1619

1620 **G HYPERPARAMETER TUNING STRATEGY**
16211622 In our experiments, the hyperparameters were tuned individually for each combination of method,
1623 dataset, and random seed.
16241625 Table 1: Hyperparameter tuning strategy for each method.
1626

FedAvg	Stepsize	Grid search over {0.1, 0.01, 0.001}
FedAvg (Adam)	Stepsize	Grid search over {0.1, 0.01, 0.001}
SCAFFOLD	Stepsize	Grid search over {0.1, 0.01, 0.001}
SCAFFOLD (Adam)	Stepsize	Grid search over {0.1, 0.01, 0.001}
LocalMuon	Stepsize of Muon	Grid search over {0.001, 0.0001}
	Stepsize of Momentum SGD	Grid search over {0.1, 0.01}
FedMuon	Stepsize of Muon	Grid search over {0.001, 0.0001}
	Stepsize of Momentum SGD	Grid search over {0.1, 0.01}

1635 In the following tables, we list the hyperparameters tuned by the grid search. The reported hyper-
1636 parameters correspond to the values selected from two independent trials with different random
1637 seeds.
16381639 Table 2: Hyperparameters tuned for FashionMNIST.
1640

	$\beta = 10.0$	$\beta = 0.1$
FedAvg	{0.1, 0.1}	{0.1, 0.1}
FedAvg (Adam)	{0.1, 0.1}	{0.01, 0.01}
SCAFFOLD	{0.1, 0.1}	{0.1, 0.1}
SCAFFOLD (Adam)	{0.001, 0.001}	{0.001, 0.001}
LocalMuon	{(0.001, 0.1), (0.001, 0.01)}	{(0.001, 0.1), (0.001, 0.1)}
FedMuon	{(0.001, 0.01), (0.001, 0.01)}	{(0.001, 0.01), (0.001, 0.01)}

1649 Table 3: Hyperparameters tuned for CIFAR-10.
1650

	$\beta = 10.0$	$\beta = 0.1$
FedAvg	{0.1, 0.1}	{0.1, 0.1}
FedAvg (Adam)	{0.001, 0.001}	{0.01, 0.001}
SCAFFOLD	{0.1, 0.1}	{0.1, 0.1}
SCAFFOLD (Adam)	{0.001, 0.001}	{0.001, 0.001}
LocalMuon	{(0.001, 0.01), (0.001, 0.01)}	{(0.001, 0.01), (0.001, 0.01)}
FedMuon	{(0.001, 0.01), (0.001, 0.01)}	{(0.001, 0.01), (0.001, 0.01)}